HHS Public Access

Author manuscript

Food Chem Toxicol. Author manuscript; available in PMC 2025 April 01.

Published in final edited form as:

Food Chem Toxicol. 2024 April ; 186: 114578. doi:10.1016/j.fct.2024.114578.

Systemic and immunotoxicity induced by topical application of perfluorohexane sulfonic acid (PFHxS) in a murine model

Lisa M. Weatherly[*], **Hillary L. Shane**, **Laurel G. Jackson**, **Ewa Lukomska**, **Rachel Baur**, **Madison P. Cooper**, **Stacey E. Anderson**

Allergy and Clinical Immunology Branch, Health Effects Laboratory Division, National Institute for Occupational Safety and Health, Morgantown, WV, USA

Abstract

Per- and polyfluoroalkyl substances (PFAS) are a large group of stable synthetic surfactants that are incorporated into numerous products for their water and oil resistance and have been associated with adverse health effects. The present study evaluated the systemic and immunotoxicity of sub-chronic 28- or 10-day dermal exposure of PFHxS (0.625–5% or 15.63–125 mg/kg/dose) in a murine model. Elevated levels of PFHxS were detected in the serum and urine, suggesting that absorption is occurring through the dermal route. Liver weight (% body) significantly increased and spleen weight (% body) significantly decreased with PFHxS exposure, which was supported by histopathological changes. Additionally, PFHxS significantly reduced the humoral immune response and altered immune subsets in the spleen, suggesting immunosuppression. Gene expression changes were observed in the liver, skin, and spleen with genes involved in fatty acid metabolism, necrosis, and inflammation. Immune-cell phenotyping identified significant decreases in B-cells, NK cells, and $CD11b^+$ monocyte/macrophages in the spleen along with increases in $CD4^+$ and $CD8^+$ T-cells, NK cells, and neutrophils in the

[*]Corresponding author. National Institute for Occupational Safety and Health (NIOSH), 1095 Willowdale Drive, Morgantown, WV, 26505, USA. nux6@cdc.gov (L.M. Weatherly).

CRediT authorship contribution statement

Lisa M. Weatherly: Writing – review & editing, Writing – original draft, Methodology, Investigation, Formal analysis, Conceptualization. **Hillary L. Shane:** Writing – review & editing, Methodology, Investigation, Formal analysis, Conceptualization. **Laurel G. Jackson:** Writing – review & editing, Methodology, Investigation. **Ewa Lukomska:** Writing – review & editing, Resources, Investigation. **Rachel Baur:** Writing – review & editing. **Madison P. Cooper:** Writing – review & editing, Methodology, Investigation. **Stacey E. Anderson:** Writing – review & editing, Supervision, Methodology, Investigation, Funding acquisition, Formal analysis, Conceptualization.

Declaration of competing interest

The authors declare that they have no known competing financial interests or personal relationships that could have appeared to influence the work reported in this paper. The authors alone are responsible for the content of this manuscript. The findings and conclusions in this report are those of the authors and do not necessarily represent the official position of the National Institute for Occupational Safety and Health, Centers for Disease Control and Prevention. All study data will be made available on the NIOSH Data and Statistics Gateway.

Appendix A. Supplementary data

Supplementary data to this article can be found online at https://doi.org/10.1016/j.fct.2024.114578.

skin. These findings support dermal PFHxS-induced liver damage and immune suppression. Overall, data support PFHxS absorption through the skin and demonstrate immunotoxicity via this exposure route, suggesting the need for further examination.

Keywords

Perfluorohexane sulfonic acid (PFHxS); Toxicity; Immune; Dermal; Liver damage; Ppar; Immunosuppression

1. Introduction

Per- and polyfluoroalkyl substances (PFAS) are a large group of stable synthetic surfactants with unique chemical and physical properties including water and oil resistance, heat and corrosion stability, and solubility (Lau et al., 2007). Due to these properties, PFAS have been used in the manufacturing of both consumer and industrial products (food packaging, textile coatings, fire-retardant foams, cleaners, wood glue, ski wax, leather, nonstick cookware, carpets, etc.) (Kotthoff et al., 2015; Lindstrom et al., 2011). However, these properties due to their strong carbon-fluorine bond, make these chemicals resistant to degradation (Wang et al., 2017) and allow them to accumulate in the environment and in humans (Calafat et al., 2007; Lau et al., 2007), leading to environmental and human health concerns.

The two most widely known and studied PFAS are perfluorooctanesulfonic acid (PFOS) and perfluorooctanoic acid (PFOA); they have an 8-carbon structure and are considered legacy compounds. PFOS and PFOA have been detected in human whole blood and serum samples in the United States and throughout the world (Lau et al., 2007). A science panel focusing on PFOA (also known as C8 by the panel) exposure from a DuPont plant in Parkersburg, WV reported probable links between PFOA exposure and thyroid disease, high cholesterol, kidney and testicular cancer, and pregnancy-induced hypertension (C8 science panel). Many studies have investigated the hepatic effects of PFAS (focused mainly on PFOA and PFOS) in both rodents and humans, observing steatosis, lipid accumulation, elevated alanine transaminase (ATL) levels and associations with alterations in triglycerides, bilirubin, and uric acid (Costello et al., 2022).

Another PFAS that is highly detected in human samples is perfluorohexane sulfonic acid (PFHxS), which has a 6-carbon chain. The 3M Company was the main U.S. manufacturer of PFOS, PFOA, and PFHxS, however, the company discontinued the production of these compounds between 2000 and 2002. Although PFHxS has been phased out of most production in the U.S., exposure is still of concern as it is produced in other countries, and it is not easily degraded in the environment. Also, PFHxS has a long half-life of 4.7–35 years in humans, a longer half-life than both PFOS (3.3–27 years) and PFOA (2.1–10.1 years) (ATSDR, 2021). In human serum samples, PFHxS had the highest degree of stability of the compounds tested, including PFOS and PFOA, over the 1–5- and 10–18-year periods investigated (Blake et al., 2018). PFHxS was still detected in humans in a 2003–2004 study, several years after its production was discontinued. In a Norwegian study, PFHxS concentration actually increased in human blood samples between 2007/2008 to 2013/2014 (Poothong et al., 2017). Associations have been observed between PFHxS serum

concentrations and changes in cholesterol in humans (Fisher et al., 2013; Nelson et al., 2010; Yang et al., 2018). Animal studies with PFHxS exposure via gavage have resulted in an increase in liver weight, steatosis, enlargement of hepatocytes, and alterations in serum cholesterol (Butenhoff et al., 2009; Chang et al., 2018; Das et al., 2017).

While oral PFAS exposure is the most widely studied, there is the potential for dermal exposure via commercial products, the environment, and occupationally. PFAS exposure can occur to the general population via consumer products (mentioned above) (Kotthoff et al., 2015) through which dermal exposure could occur to both the consumer and the manufacturers (during the production process) of these products. PFAS have also been detected in surface water, sea water, drinking water, waste water, and soils (Lau et al., 2007). Several occupations undergo exposure to PFAS, such as firefighters and support services, ski wax technicians, cleanup workers, and PFAS manufacturing workers (Freberg et al., 2010; Plassmann and Berger, 2013; Trowbridge et al., 2020; USEPA, 2022). While data describing exposure to PFAS is limited in most occupational settings, firefighter exposure to PFHxS has been characterized in a number of studies. Firefighters can be exposed to PFAS via multiple routes (including dermal) through release of consumer products during burning, use of fire-fighting foams, and use of PFAS coated firefighting equipment (Laitinen et al., 2014; Maizel et al., 2023; Peaslee et al., 2020). Dust samples from fire stations in Massachusetts detected PFAS in 92.3% of the samples, supporting potential dermal exposure (Young et al., 2021). U.S. male and female firefighters were found to have higher PFHxS serum concentrations when compared to workers in other job categories (Jin et al., 2011; Trowbridge et al., 2020). In U.S. firefighters, PFHxS serum concentrations were ~50% higher than the general population (Khalil et al., 2020) and higher PFHxS serum concentrations were observed (compared to the general population) in all fire departments tested (Burgess et al., 2023). A recent review paper provides additional support that firefighters consistently have elevated serum levels of PFAS, including PFHxS (Rosenfeld et al., 2023).

PFAS have also been linked to immune function alterations in humans. In an epidemiology study from 2008 to 2011, incidence of ulcerative colitis was significantly increased in association with PFOA serum levels (Steenland et al., 2013). In the National Health and Nutrition Examination Survey 2007–2010, a statistically significant association with serum PFOA, PFOS, and PFHxS and higher odds of self-reported food allergies were observed (Buser and Scinicariello, 2016). A study done in Northern Norway found that higher PFOS and PFHxS serum concentrations were associated with higher odds of asthma (Averina et al., 2019). Many i*n vivo* animal model studies have also investigated PFAS' impacts on immune function, showing alterations in lymphocytic subpopulations, decreased natural killer cell activity, cytokine level alterations, decreased IgM levels, decreased plaque-forming cell response, and decreased antigen-specific antibody response (De Guise and Levin, 2021; DeWitt et al., 2016; Dong et al., 2009; Zheng et al. 2009, 2011). The majority of these studies were done with either PFOS or PFOA, with fewer studies evaluating the effects of PFHxS on immune function. Also, all these *in vivo* study exposures occurred through oral exposure with limited research exploring other routes of exposure.

Our lab has previously shown that multiple PFAS (Shane et al., 2020; Weatherly et al., 2021, 2023) are absorbed through the skin, leading to functional immune effects and systemic

toxicity. A recent review on PFAS dermal uptake states that although many studies have found products that contain PFAS come into contact with the skin, the knowledge of PFAS dermal uptake is lacking (Ragnarsdóttir et al., 2022). To help fill in this knowledge gap, the present study aims to investigate immunotoxicity and systemic effects of sub-chronic dermal exposure of PFHxS in a murine model. These experiments are needed to fill research gaps identified for these compounds and to fully understand the health effects following the dermal route of exposure.

2. Materials and methods

2.1. Animals

Female $B_6C_3F_1$ mice were used in these studies as they are the National Toxicology Program preferred strain for evaluating general toxicity and have been used previously to investigate PFAS immunotoxicity (Shane et al., 2020; Weatherly et al., 2021, 2023). All mice were purchased from Jackson Laboratory (Bar Harbor, ME) at 7–8 weeks of age. Upon arrival, the animals were allowed to acclimate for a minimum of 5 days. All animals were randomly assigned to treatment groups, weighed, and individually identified via tail marking using a permanent marker. Dose groups were identified by cage cards. Both the dosing group as well as the animal numbers were identified on each cage. The animals were housed 5 mice/cage in ventilated plastic shoe box cages with hardwood chip bedding, modified NIH-31 6% irradiated rodent diet (Harlan Teklad – item #7913) and sterile tap water from water bottles *ad libitum*. The temperature in the animal facility was maintained between 65 and 78 °F and the relative humidity between 30 and 70%; a light/dark cycle was maintained at 12-hr intervals. All animal experiments were performed in an AAALAC International accredited National Institute for Occupational Safety and Health (NIOSH) animal facility in accordance with an animal protocol approved by the CDC-Morgantown Institutional Animal Care and Use Committee. This activity was reviewed by CDC, deemed research not involving human subjects, and was conducted consistent with applicable federal law and CDC policy.

2.2. Test articles and chemicals

Acetone [CAS #67–64-1] was purchased from Sigma-Aldrich. Perfluorohexane sulfonic acid (95%, PFHxS) [CAS #355–46-4] was purchased from Synquest Laboratories.

2.3. PFAS exposures

To evaluate systemic and immunotoxicity, $B_6C_3F_1$ mice (5/group) were topically treated on the dorsal surface of each ear (25 μl/ear) with vehicle (acetone) or PFHxS concentrations (1.25, 2.5, 5% w/v) once a day for 28 consecutive days. Five mice per group have previously been shown to be sufficient to obtain statistical significance. These studies were conducted for the purpose of hazard identification and the concentrations of PFHxS were selected based on an initial 7-day range finding study and previous studies conducted with various PFAS (Shane et al., 2020; Weatherly et al., 2023). Body weights were measured weekly before exposure to ensure no overt toxicity was occurring due to PFAS exposure. Animals were euthanized by CO_2 asphyxiation approximately 24 h after the last exposure.

For the immune function studies, $B_6C_3F_1$ mice (5/group) were topically treated on the dorsal surface of each ear (25 μl/ear) with vehicle (acetone) or PFHxS concentrations (0.625, 1.25, 2.5% w/v) once a day for 10 consecutive days. A lower PFHxS concentration and fewer days of exposure were used in these studies as no trends in weight loss was observed by day 10 with these lower concentrations (data not shown). Four days prior to euthanasia, the mice were immunized with 7.5×10^7 Sheep Red Blood Cells (SRBC) (in 200 μl volume) by i.v. injection. Blood for these studies were drawn from a single donor animal (Lampire Laboratories; Pipersville, PA). Animals were euthanized by CO_2 asphyxiation approximately 24 h after the last exposure.

2.4. Tissue processing

Following euthanasia, animals were weighed, and examined for gross pathology. The liver, spleen, kidneys, and thymus were removed, cleaned of connective tissue, and weighed. Left and right auricular draining lymph nodes (dLNs; draining the site of chemical application), spleen (1/2), and one ear pinna were collected and placed in 4 mL RPMI (Corning). Spleen (1/2), dLN (2 nodes/animal), and ear (1) pinna single cell suspensions for immune phenotyping were prepared as previously described (Weatherly et al., 2021). Half of one ear pinna was placed in 0.5 mL of RNAlater for subsequent gene expression analysis (see below). A small lobe of the liver (caudate) was collected in 0.5 mL of RNAlater for subsequent gene expression (see below). The remainder of the liver, spleen (1/2), ear pinna (1/2), and one kidney (right) were collected in 10% formalin for histopathology analysis.

2.4.1. Serum chemistries—Blood samples were collected via cardiac puncture, transferred to serum separation tubes, and separated by centrifugation. The serum was frozen at −20 °C for subsequent serum chemistry analysis. Selected serum chemistries were evaluated using a Catalyst DX Chemistry Analyzer (IDEXX Laboratories, Inc.; Westbrook, ME). Endpoints analyzed included: alkaline phosphates (ALKP), urea nitrogen (BUN), glucose (GLU), and cholesterol (CHOL).

2.4.2. Analytical PFAS detection—Serum and urine samples were collected and analyzed for PFHxS by Vista Analytical Laboratory, following Vista's standard operating procedures (Vista Analytical Laboratory, El Dorado Hills, CA) of solid phase extraction and liquid chromatography/tandem mass spectrometry (LC/MS/MS) using BEH C18 columns as described in (Shoemaker et al., 2008). Vista Analytical follows EPA method 537. An aliquot of serum was collected (as described above) from each animal and urine was pooled following euthanasia for each group of mice. The results for PFHxS include the linear isomer only. The Initial Calibration and Continuing Calibration Verifications met the acceptance criteria as described in (Shoemaker et al., 2008). No analytes were detected in the Method Blank above Reporting Limit (200 ng/mL). The labeled standard recoveries for all quality controls and samples were within the acceptance criteria as described in (Shoemaker et al., 2008).

2.4.3. Flow cytometry—Flow cytometry was conducted as previously described (Weatherly et al., 2021). For staining, single cell suspensions were resuspended in staining buffer containing anti-mouse CD16/32 antibody (Fc Block; BD Biosciences) then incubated

with a cocktail of fluorochrome-conjugated antibodies specific for mouse cell surface antigens. For dLN and spleen cells: B220–V500 (RA3–6B2), CD11b-PerCP-Cy5.5 (M1/70), CD8-PE-CF594 (53–6.7), Siglec-F-PE (E50–2440), Ly6G-FITC (1A8) (BD Biosciences), CD11c-eFluor 450 (N418), CD86-APC (GL1) (eBioscience), CD45-Superbright 780 (30-F11), F4/80-PE-Cy7 (BM8), MHCII-APC-eF780 (M5/114.15.2) (Invitrogen), CD4-BV711 (RM4–5), Ly6C-AF700 (HK1.4) (BioLegend). For ear pinna cells: CD4-BV711 (RM4–5), NKp46-BV605 (29A1.4) (BioLegend), CD8-PE-CF594 (53–6.7), CD3-V500 (500A2), Ly6G-FITC (1A8), CD11b-PerCP-Cy5.5 (M1/70), CD11c-AF700 (HL3), Siglec-F-PE (E50–2440) (BD Biosciences), F4/80-PE-Cy7 (BM8), MHCII-APC-eF780 (M5/114.15.2), CD45-Superbright 780 (30-F11), FcεRI-APC (MAR-1) (Invitrogen), CD117-eFluor 450 (2B8) (eBioscience). Ear total cellularity was determined using a Cellometer with AO/PI (Nexcelom) and dLN and spleen total cellularity was determined using a Z2 Coulter Particle Count and Size Analyzer (Beckman Coulter). Data was acquired on a LSR II flow cytometer (BD Biosciences) and analyzed using FlowJo v10 software (TreeStar Inc., Ashland, OR). Cellular populations were defined using the gating strategies outlined in Supplemental Table 1; Fluorescence minus ones (FMOs) were used as gating controls. An example of gating strategies for dLN, spleen and ear are outline in Supplemental Figs. 1 and 2.

2.4.4. Gene expression—Ear (half an ear pinna/mouse) and liver (caudate) were homogenized on a TissueLyser II in Buffer RLT (Qiagen). Total RNA was isolated using Qiagen's RNeasy mini spin column kits with DNase treatment on a QIAcube automated RNA isolation machine. RNA concentrations and purity were analyzed on a NanoDrop spectrophotometer (Thermo Fisher Scientific). The cDNA (1–2 μg) was prepared on an Eppendorf Mastercycler using Applied Biosystems' High Capacity Reverse Transcription kit. The cDNA was used on the real-time RT^2 Profiler PCR Array Mouse Immunotoxicity Targets (QIAGEN; Product #: PAMM-179ZC) and Innate and Adaptive Immune Response (QIAGEN; Product #: PAMM- 052ZC) (spleen) and peroxisome proliferator-activated receptor (PPAR) Targets and Hepatoxicity (QIAGEN; Product #: PAMM-149ZC and PAMM-093ZC) (liver) and also used as template for real-time PCR reactions containing TaqMan PCR Master Mix with gene-specific primers (Applied Biosystems) on a 7500 Real-Time PCR System. Transcripts were chosen to be confirmed via TaqMan qPCR based on fold- change and number of concentrations that were altered (gene list Supplemental Table 2). Relative fold gene expression changes ($2^{-\Delta\Delta CT}$) were determined compared to vehicle controls and normalized for expression of reference gene β-actin (Taqman) or β2-microtubulin, Gapdh, and Hsp90ab1 (PPAR and Hepatoxicity arrays).

2.4.5. Histology—Each tissue sample stored in 10% formalin was embedded in paraffin, sectioned at 5 μm, stained with hematoxylin and eosin (H&E) and evaluated by a veterinary pathologist at StageBio (Mason, Ohio) using The Society of Toxicologic Pathology Guideline (Crissman et al., 2004). Provantis™ pathology software v10.2.3.1 was utilized for data capture and table generation. Histopathology grades were assigned as grade 1 (minimal), grade 2 (mild), grade 3 (moderate), grade 4 (marked), or grade 5 (severe) based on an increasing extent of change. Criteria used for skin grading was previously described (Weatherly et al., 2021).

2.5. Spleen IgM response to SRBC

The primary IgM response to SRBC was enumerated using a modified hemolytic plaque assay (Jerne and Nordin, 1963; Shane et al., 2020). Four days prior to euthanasia, the mice were immunized with 7.5×10^7 SRBC (in 200 µl volume) by i.v. injection. On the day of sacrifice, mice were euthanized by CO_2 asphyxiation, body and organ weights were recorded, and spleens were collected in 3 mL of Hank's balanced salt solution (HBSS). Single cell suspensions of the spleens from individual animals were prepared in HBSS by disrupting the spleen between the frosted ends of microscopic slides. To identify the total number of spleen cells, 20 µl of cells were added to 10 mL of Isoton II diluent (1:500; Beckman Coulter, Brea, CA) and two drops of Zap-o-globin (Beckman Coulter, Brea, CA) were added to lyse red blood cells. Cells were then counted in the Coulter counter. Dilutions (1:30 and 1:120) of spleen cells were then prepared and 100 µl of each dilution were added to test tubes containing a 0.5 mL warm agar/dextran mixture (0.5% Bacto-Agar, DIFCO; and 0.05% DEAE dextran; Sigma, St. Louis, MO), 25 µl of 1:1 ratio of SRBC suspension, and 25 µl of 1:4 dilution (1 mL lyophilized) guinea pig complement (Cedarlane Labs, Burlington, Canada). Each sample was vortexed, poured into a Petri dish, covered with a microscope coverslip, and incubated for 3 h at 37 °C. The plaques (representing antibody-forming B-cells) were then counted. Results were expressed in terms of both specific activity (IgM PFC per 10^6 spleen cells) and total activity (IgM PFC per spleen).

2.5.1. Serum IgM response to SRBC—Serum samples were analyzed for anti-SRBC IgM using a commercially available ELISA kit (Life Diagnostics, West Chester, PA), according to manufacturer recommendations with modifications. In brief, test serum was diluted (1:40, 1:80, 1:160, and 1:320) and incubated in the anti-SRBC coated microtiter wells for 45 min at 25 °C. The wells were subsequently washed, 100 µl horseradish peroxidase-conjugated secondary antibody was added and the plates incubated for an additional 45 min at 25 °C. Thereafter, the wells were washed to remove unbound antibodies and 100 µl tetramethylbenzidine peroxidase (TMB) reagent was added to each well. The plates were incubated for 20 min at room temperature before color development was stopped by addition of 50 µl of kit-provided Stop Solution. Optical density in each well was then measured spectrophotometrically at 450 nm using a Spectra Max Plus plate reader (Molecular Devices, Sunnyvale, CA). The concentration of anti-SRBC IgM in the test samples was determined by comparison to a standard curve generated in parallel using SoftMax Pro software and reported as units of anti-SRBC IgM (U/ml) plotted vs absorbance values at 450 nm.

2.6. Statistical analysis

A one-way analysis of variance (ANOVA) was conducted for analysis of the data generated from the described animal studies. If the ANOVA showed significance at $p \leq 0.05$, the Dunnett's Multiple Range *t*-test was used to compare treatment groups with the control group. Kruskal-Wallis with Dunn's post-test was conducted for gene expression analysis in groups that had unequal variances. Linear trend test was also conducted to show a dose response in select endpoints tested. No correction for multiple endpoints has been applied. Statistical analysis was performed using Graph Pad Prism version 9.2 (San Diego, CA).

Results represent the mean ± SE of 5 mice per group. Statistical significance is designated by *p ≤ 0.05, **p ≤ 0.01, and ***p ≤ 0.001.

3. Results

3.1. 28-Day dermal exposure of PFHxS induced significant alterations in both serum and urine PFHxS concentration

A statistically significant dose-dependent increase in PFHxS serum concentration was observed with 1.25, 2.5, and 5% PFHxS (Fig. 1A), increasing from 1.22 μg/mL (control) to 440 μg/mL, 608 μg/mL, and 656 μg/mL, respectively. This suggests that there is consequential absorption occurring after PFHxS dermal exposure. Statistical analysis could not be performed on urine samples as each concentration is 5 pooled samples with a single data point. Urine PFHxS concentration increased from a non-detectable level to 43 μg/mL with 1.25%, 120 μg/ mL with 2.5%, and 130 μg/mL with 5% (Fig. 1B).

3.2. Dermal exposure of PFHxS for 28 days results in significant changes in organ weight

After 28-days of PFHxS exposure there was a statistically significant increase in liver weight (as a % of body weight) (Fig. 2A). Liver weight significantly increased following exposure to 1.25, 2.5, and 5% PFHxS (162%, 172%, and 205%, respectively, vs. values for vehicle-treated mice). Spleen weights (% of body) were significantly decreased for all three PFHxS concentrations (Fig. 2C), decreasing by 25%, 37%, and 38% with 1.25, 2.5 and 5% PFHxS, respectively. Thymus weight (% of body) also decreased with 2.5 and 5% PFHxS (44% and 47%, respectively) (Fig. 2D). No change in weights (as a % of body weight) was observed in the kidney (Fig. 2B). A significant decrease in body weight (14%) did occur with 5% PFHxS exposure (Supp. Fig. 3). This decrease in body weight could indicate a decrease in nutritional (caloric) intake by the mice. Although overt toxicity (loss of greater than 10% body weight) occurred with 5% PFHxS, the significant changes in organ weights were dose dependent (significant linear trend $p < 0.001$) and observed in the absence of overt toxicity (1.25% and 2.5%). Organ weight not corrected for total body weight are reported in Supplemental Table 3, with significant increases in mass of liver (1.25, 2.5, 5% PFHxS doses) and significant decreases in mass of thymus, spleen, and kidneys (1.25, 2.5, 5% PFHxS doses).

3.3. Dermal exposure of PFHxS altered serum chemistry

A significant increase in serum alkaline phosphatase (ALKP) and alanine aminotransferase (ALT) and a significant decrease in cholesterol, glucose, and urea nitrogen (BUN) was observed following 28-day PFHxS exposure (Fig. 3). Cholesterol and BUN decreased at 2.5 and 5% PFHxS with cholesterol decreasing by 43% and BUN decreasing by 34% with 5% PFHxS (Fig. 3 A, D). Glucose decreased at all three PFHxS concentrations with 5% PFHxS causing a decrease of 58% (Fig. 3B). ALKP increased with 2.5% PFHxS (87%) and 5% PFHxS (161%) (Fig. 3C) and ALT increased with 5% (360%) (Fig. 3E). The significant changes in serum chemistries were dose dependent [significant linear trend $p < 0.001$ (cholesterol, glucose, ALKP), $p < 0.01$ (BUN), $p < 0.05$ (ALT)] and/or observed in the absence of overt toxicity.

3.4. Dermal exposure of PFHxS for 28 days results in histopathological changes in the liver, kidney, and spleen

In the liver, histopathological examination revealed that PFHxS induced marked hepatocellular hypertrophy in all 5 animals with all three PFHxS exposures (Table 1). Hepatocellular hypertrophy was characterized by increased cytoplasmic eosinophilia, decreased glycogen content, often minimal peripherally located clear vacuoles, and diffusely increased cellular volume of hepatocytes. Hypertrophy of hepatocytes distorted the hepatic architecture. Individual animals treated with 1.25% PFHxS displayed minimal (3/5) and mild (2/5) necrosis, 5/5 mice showed increased bile, 4/5 exhibited minimal pigmented macrophages, and 2/5 showed minimal and 1/5 showed a mild decrease in incidence of mononuclear infiltrates (Table 1). Increased bile was characterized by small amounts of golden-brown, finely granular pigment within the hepatocyte cytoplasm. Pigmented macrophages were present in the sinuses singly and in small accumulations and contained a similar granular golden-brown pigment consistent with bile. Hepatocyte necrosis was most often consistent with apoptosis (single cell necrosis) and was characterized by cellular shrinkage, rounding and karyorrhectic nuclei; however, rare cells had loss of cytoplasmic integrity (necrosis) with leukocyte infiltrates. Animals treated with 2.5% PFHxS induced minimal (4/5) and mild (1/5) necrosis, minimal increased bile (5/5), minimal pigmented macrophages (5/5) and minimal decrease in mononuclear infiltrates (2/5) (Table 1). With 5% PFHxS 4/5 mice displayed minimal necrosis and 1/5 mild necrosis, 5/5 mice showed increased bile, 4/5 displayed pigmented macrophages, and 1/5 decreased in mononuclear infiltrates (Table 1; Fig. 4B).

In the kidney, minimal infiltrates of mononuclear cells were noted in 4/5 control animals, but none were observed in any of the animals administered any of the three PFHxS concentrations (Table 1; Fig. 4C and D). In the spleen of animals exposed to PFHxS, mildly decreased lymphocyte cellularity was characterized by overall decreased size of lymphoid aggregates in the white pulp. A mild decrease in lymphocyte cellularity was observed with 1.25% PFHxS (2/5 mice), 2.5% (4/5 mice), and 5% (5/5 mice) (Table 1; Fig. 4E and F). This finding had a dose response in incidence and correlated with decreased spleen weight parameters. No microscopic abnormalities were noted in the skin at the dosing site (data not shown).

3.5. Dermal PFHxS exposure results in changes in liver and skin gene expression

To further investigate the mechanism of PFHxS systemic toxicity, two PCR pathway-based arrays were also investigated with liver mRNA. Multiple genes in hepatoxicity and PPAR target arrays were significantly altered (Supp. Table 4). Genes involved in cholestasis (*Abcb1, Abcc3, Rdx*), steatosis (*Cd36, Lpl, Srebf1*), phospholipidosis (*Abcb1*), hepatoxicity (*Aldoa, Avpr1a, Bhmt, Car3, Cxcl12, Fads1, Fmo1, Gclc, Gsr, Igfals, Krt18, Maob, Mbl2, Pla2g12a, Pygl, Thrsp*), necrosis (*Fam214a, Mlxipl*), adipogenesis (*Nr1h3*), fatty acid metabolism (*Acadl, Acadm, Acox1, Acox3, Cpt1b, Cyp27a1, Cyp4a10, Cyp7a1, Ehhadh*), lipid transport (*Angptl4, Apoa1, Apoa5, Apoc3, Nr1h3*), PPAR cofactors (*Helz2, Chd9, Creb1, Ncoa3, Ppargc1a, Sirt1, Smarcd3, Tgs1*), PPAR ligand transport (*Lpl, Slc22a5, Slc27a5*), and PPAR transcription factors (*Pparδ, Pparγ, Rxrg*) were altered at all three PFHxS concentrations (Supp. Table 4). Transcripts were chosen to be confirmed via TaqMan

qPCR based on fold-change and number of concentrations that were altered. Increases in gene expression were observed at all three PFHxS concentrations of *Acox1, Cd36, Lpl*, and *Ehhadh* with fold increases at 5% PFHxS of 6.7- fold, 23-fold, 30-fold, and 61-fold, respectively (Fig. 5A–D). Large increases were also seen in *Serpine1* (2.5%, 52-fold), *Cpt1b* (5%, 33-fold), *Cyp4a10* (5%, 22-fold) and *Pla2g12a* (5%, 16-fold) (Fig. 5E–H). Decreases in gene expression were observed with *Apoa1* (2.5%), *Avpr1a* (5%), and *Cyp7a1* (1.25%) (Fig. 5I–K). No change was observed in *Pparα*, while a decrease in *Pparδ* occurred at 1.25% and 2.5% PFHxS, and an increase in *Pparγ* at 1.25% and 5% (Fig. 5L–N). The significant changes in liver gene expression were dose responsive [significant linear trend $p < 0.001$ (*Acox1, Lpl, Ehhadh, Cpt1b, Cyp4a10, Pla2g12a, Avpr1a*), $p < 0.01$ (*Cd36, Apoa1, Pparδ*), $p < 0.05$ (*Cyp7a1*)] and/or observed in the absence of overt toxicity.

Gene expression of the skin was conducted to help define the mechanism of PFHxS systemic and immunotoxicity. Although in the absence of histological changes, inflammatory cytokine, *Il-6*, increased (2-fold) with 5% PFHxS exposure (Fig. 6B); no significant changes were observed with *Il-1β* (Fig. 6A). Gene expression of *Tslp* (Th2 skewing cytokine), *Cxcl1* (chemokine), and *S100a8* (danger-associated molecular pattern) also increased with 5% PFHxS (33-fold, 5-fold, 9-fold, respectively) (Fig. 6C, D, F). *Serpine1*, involved in necrosis, increased at 1.25%, 2.5%, and 5% PFHxS (3-fold, 4-fold, 4-fold, respectively) (Fig. 6E). In the skin, no change was observed in *Pparα* gene expression, but an increase was seen in *Pparδ* and a decrease with *Pparγ*, both at 5% PFHxS (Fig. 6G–I). Increases were seen in 2 skin barrier genes, *Lor* (2.5%, 5%) and *Flg* (5%), after 28-days PFHxS exposure (Fig. 7C and D). No changes were seen in the skin barrier genes *Flg2, Itgbl1, Krt10*, and *Krt14*. The significant changes in skin gene expression were dose responsive [significant linear trend $p < 0.001$ (*Cxcl1, Flg*), $p < 0.01$ (*Il-6, Tslp, Serpine1, Pparδ, Pparγ, Lor*), $p < 0.05$ (*S100a8*)] and/or observed in the absence of overt toxicity.

3.6. Dermal exposure of PFHxS for 28 days results in significant phenotypic changes in the skin

Phenotypic analysis of the ear pinna following 28 days of PFHxS exposure resulted in increases in number and frequency of $CD45^+$ cells (5%), $CD4^+$ T cells (2.5%, 5%), $CD8^+$ T cells (2.5%, 5%), neutrophils (5%), and $CD11b^+$ DCs (5%) (Table 2). Decreases in number and frequency were observed with NK cells (2.5%, 5%) and $CD11b^-$ DCs (1.25%, 2.5%, 5%). An increase in eosinophil and macrophage number occurred with 5% PFHxS (Table 2).

Fewer changes were observed in the dLN, showing a significant decrease in $CD4^+$ T cell number with 1.25%, 2.5%, and 5% PFHxS. An increase in $CD8^+$ T cell frequency (2.5%, 5%), eosinophil frequency and number (2.5%, 5%), total DC number (5%), mean fluorescence intensity of MHCII and CD86 on B cells (5%) was observed with PFHxS exposure (Supp. Table 5).

3.7. Dermal PFHxS exposure results in significant changes in spleen phenotyping and gene expression

Consistent with the decrease in organ weight, PFHxS dermal exposure induced a decrease in total cellularity after 28 days of exposure in the spleen with 2.5% and 5% PFHxS (Table

3). A decrease in B-cell number (2.5%, 5%) and frequency (5%) also occurred with PFHxS exposure. PFHxS also induced a decrease in frequency and number in NK cell (2.5%, 5%), eosinophils (1.25%, 2.5%, 5%), $CD11b^+$ cells (2.5%, 5%), $CD11b^+Ly6C^+$ cells (2.5%, 5%), and $CD11b^+Ly6C^-$ cells (1.25%, 2.5%, 5%). $CD4^+$ and $CD8^+$ T cells (2.5%, 5%) and total dendritic cells (5%) decreased in number. $CD4^+$ and $CD8^+$ T cells increased in frequency (2.5%, 5%) along with neutrophils (5%). Mean fluorescence intensity of MHCII decreased on both B cells and DCs (Table 3).

To further investigate immunotoxicity in the spleen, gene expression was also evaluated. Two PCR pathway-based arrays were investigated with spleen mRNA (Immunotoxicity and Innate & Adaptive Immune Responses arrays). Genes involved in immunotoxicity (*Agcg1, Mup3, Serpina3m, Btnl10, Cdr2, Crim1, Ctse*), inflammatory response (*Serpina3m*), immune response (*Ctse, Cebpb*), unfolded protein response (*Cebpb, Chac1*), cell cycle (*Fbxo38*), transcription factors (*Cebpb, Id1*), innate immunity (*C5ar1, Mpo, Stat1, Tlr5, Tlr6, Tlr7, Tlr8*) and adaptive immunity (*Ifngr1, Stat1, Cxcl10*) were altered (Supp. Table 4). Transcripts with the highest fold changes were confirmed via TaqMan qPCR. All Tlr's assayed increased (*Tlr5, 6, 7, 8*) in expression along with *Il-10* and *Crim1, Chac1, Fbxo38, Id1*, and *Abcg1* and a decrease in *Ctse* was observed (Fig. 8A–K). The significant changes in spleen gene expression were dose responsive [significant linear trend $p < 0.001$ (*Tlr5, Crim1, Ctse, Chac1, Fbxo38, Id1, Abcg1*), $p < 0.01$ (*Tlr6, Tlr7, Tlr8, Il-10*)] and/or observed in the absence of overt toxicity.

3.8. Dermal exposure of PFHxS suppresses the adaptive immune response

To evaluate if dermal exposure to PFHxS was immunosuppressive, the murine IgM response to SRBC was examined following a 10-day exposure to PFHxS. PFHxS significantly reduced specific ($PFC/10^6$ cells) and total (PFC/spleen) IgM antibody activity against SRBC at 1.25 and 2.5% PFHxS exposure (Fig. 9A and B). Exposure of mice to 1.25% PFHxS resulted in a 50.7% decrease in $PFC/10^6$ cells and a 57.9% decrease in PFC/spleen vs values for vehicle-treated mice. While exposure to 2.5% PFHxS resulted in a 49.9% decrease in $PFC/10^6$ cells and a 60.3% decrease in PFC/spleen vs values for vehicle-treated mice (Fig. 9A and B). This decrease was also observed in the serum anti-SRBC IgM levels. PFHxS decreased anti-SRBC IgM levels with 0.625, 1.25, and 2.5% exposure (62.4, 51.8, 49.8% decrease, respectively) (Fig. 9C). The significant changes in spleen IgM response to SRBC were dose responsive and IgM was suppressed at non-overtly toxic concentrations. The NK assay was used to evaluate the effect of PFHxS on the innate immune system. No significant decreases in NK cell function measured using a flow-cytometric cytotoxicity assay method was observed was observed at any effector to target ratios (Supp. Fig. 4).

4. Discussion

Due to their chemical properties and ability to endure degradation, PFAS have been used as surfactants in textiles, food packaging material, and firefighting foams. However, more recent studies have found applications of PFAS to include cosmetics (makeup foundation, sunblock, etc.), personal care products, cleaning products, hand sanitizers, and makeup removers (FDA, 2022; Whitehead et al., 2021); all these applications can lead to dermal

exposure. These consumer products may also lead to occupational exposure via professional cleaning applications, beauticians, groomers, etc. Although there is the potential for dermal exposure and penetration through the skin, studies on this exposure route have not been thoroughly investigated. The current data suggest that dermal PFHxS exposure can penetrate mouse skin. Dermal exposure to 1.25–5% PFHxS resulted in detectable levels of PFHxS in the serum and the urine after 28-days of exposure. Interestingly, the current study saw much higher serum concentrations (440 μg/mL) with 1.25% (~31 mg/kg/d) PFHxS after dermal exposure compared to a study that measured serum levels after oral gavage (in *P. leucopus* or white-footed mice) where after 28 days of 20 mg/kg/d PFHxS exposure serum levels were 35 μg/mL in female mice (Narizzano et al., 2021). Other studies investigating serum concentration after oral PFHxS exposure include, female Sprague Dawley rats with a serum concentration of 42 μg/mL PFHxS after 14-days of 10 mg/kg/day PFHxS oral exposure (Butenhoff et al., 2009) and CD-1 female mice with a serum concentration of 180 μg/mL PFHxS after 14-days of 3 mg/kg/day oral PFHxS exposure (Chang et al., 2018). Our lab has previously investigated four other PFAS compounds under the same conditions and similar dermal exposure concentrations (PFBA, PFPeA, PFHxA, and PFHpA). Mice exposed to 5% PFHxA (C6) and 5% PFHpA (C7) had an average concentration of 4.8 μg/mL (serum), 1700 μg/mL (urine) and 137 μg/mL (serum), 1200 μg/mL (urine), respectively (Weatherly et al., 2023). Comparing these to the 5% PFHxS, the serum concentration was much higher (656 μg/mL) and the urine concentration much lower (130 μg/mL) with PFHxS. This data supports PFHxS having a longer half-life in female mice over PFHxA and PFHpA with dermal exposure. Few studies exist on dermal PFAS exposure. One study investigating a 2-week dermal PFHpA exposure (250 and 1000 mg/kg) in rats showed systemic changes in the kidney, liver and testes, and histopathologic lesions such as renal tubular necrosis, and hepatocellular necrosis. However, serum concentration was not measured (Han et al., 2020). A study investigating 4-day dermal PFOA exposure in BALB/c mice observed serum PFOA levels ranging from 152 ± 14 μg/mL with 0.5% PFOA to 226 ± 14 μg/mL with 2% PFOA. Also, using both *ex vivo* human full-thickness and BALB/c mouse skin revealed that the total absorbable fraction of PFOA was found to be 50% and 69% for mouse skin and full-thickness skin samples respectively (Franko et al., 2012). The same study concluded that altering the pH of the PFOA dosing solutions lead to differences in the median permeability coefficient of PFOA. Thus, PFAS ionization state needs to be considered when interpreting dermal exposure studies and could result in differing vehicles altering the permeability of PFAS.

Even though PFHxS is widely detected in the environment and in humans and has a similar structure to PFOS, fewer toxicity and immunotoxicity data exist on PFHxS. Like PFOA and PFOS, the systemic effects of PFHxS occurring after dermal exposure were mainly identified in the liver and spleen. Similar to results observed after oral PFHxS exposure (ATSDR, 2021), dermal PFHxS exposure induced a drastic increase in liver weight (162%, 172%, 205% increase with 1.25%, 2.5%, and 5% PFHxS, respectively) and hepatocyte hypertrophy. Das et al. observed ~60% increase in liver weight and hypertrophy after 7 days of 10 mg/kg PFHxS oral exposure in mice (Das et al., 2017). Mice exposed to PFHxS potassium salt (K^+PFHxS) via oral gavage for 28 days had an increase in liver weight at all concentrations tested (1.6–14 mg/kg/d) (Narizzano et al., 2023). An increase in liver weight

was also observed in male rats after 3 and 10 mg/kg/d K^+PFHxS exposure (Butenhoff et al., 2009). PFHxS exposure via oral gavage induced alterations in histopathology in mice (Chang et al., 2018). Liver dysfunction is further supported by alterations in gene expression. Metabolic dysfunction can be caused by an accumulation of fat in the liver (steatosis) and lead to an enlarged liver. *Lpl* and *Cd36* are genes involved in steatosis and were both increased ~25-fold with all three concentrations of PFHxS. PFHxS exposure also increased genes involved in fatty acid metabolism (*Acox1* and *Ehhadh*) ~6- and ~50-fold, respectively. The results observed after dermal exposure are similar to those seen after oral PFHxS exposure. Mice exposed to 3 mg/kg/d PFHxS via oral gavage showed changes in *Acox1*, *Cd36*, *Cyp4a10*, and *Ehhadh* (Chang et al., 2018). Mice fed a western-type diet with PFHxS for 4–6 weeks showed increased *Lpl*, *Cpt1b*, *Ehhadh*, and *Cd36* gene expression, and decreases in *Apoa1* and *Cyp7a1* gene expression (Bijland et al., 2011). These trends in gene expression were similar to those seen with dermal carboxylic acid PFAS exposure, however, in most cases PFHxS induced a much higher fold-change than the carboxylic acids (Weatherly et al., 2021, 2023). Further additional support for liver dysfunction is identified by significant changes in liver enzymes. ALKP and ALT were significantly increased while cholesterol, glucose and urea nitrogen were significantly decreased. APOE*3-Leiden.CETP mice that were fed a Western-type diet with K^+PFHxS for 4–6 weeks showed reduced cholesterol occurring due to impaired lipoprotein production (Bijland et al., 2011).

Inversely, dermal PFBA, PFPeA, PFHxA, and PFHpA exposure all increased glucose levels, PFBA increased cholesterol, and PFPeA, PFHxA, and PFHpA had no effect on cholesterol (Weatherly et al., 2021, 2023). Serum cholesterol can be decreased by PPARα activation (Kersten, 2008; Peters et al., 1997). Wolf et al. observed that PPARα activity (measured via luciferase assay) is more strongly activated by carboxylic acids than sulfonic acids (Wolf et al., 2008) combined with the findings that carboxylic acid PFAS have a higher affinity for PPARα than sulfonic acid (Bjork and Wallace, 2009), it is unexpected that decreases in cholesterol were observed with PFHxS while not also observed with short-chain carboxylic acid PFAS previously investigated in our lab (Weatherly et al., 2021, 2023). These findings support the need for further work to elucidate the differing effects of PFAS on lipid homeostasis and regulation on the organismal level. Although the specific activity of PPARα was not evaluated in the current study, considering that, sulfonic acids act as partial PPARα agonists (Zhao et al., 2023), there is the potential for PPARα activation. This might play a role in the decreased serum cholesterol observed in this study. On the transcriptomic level, alterations in *Pparα* gene expression have previously been observed with 14-day dermal PFOA exposure (Shane et al., 2020). Although no increase in *Pparα* gene expression was seen with dermal carboxylic acid exposure (Weatherly et al., 2021, 2023) this could be due to dynamic transcriptional regulation and mRNA turnover as *Pparα* was only assayed after the 28-day exposure.

PPARα is mainly involved in fatty acid metabolism, lipid homeostasis, and inflammation. With PFOS and PFOA, PPARα activation is thought to be a central factor in liver toxicity and dysfunction, although, PPARα-independent pathways are also suggested. Studies show that PPARα activation can mediate hepatomegaly and cholesterol after PFOS and PFOA exposure (Andersen et al., 2008). Many genes that are PPARα targets (*Cd36, Acox1, Lpl, Ehhadh, Cpt1b, Cyp4a10*) were upregulated (Rakhshandehroo et al., 2010). Although *Pparα*

gene expression was not altered after dermal PFHxS exposure, *Pparδ* was decreased with 1.25 and 2.5% PFHxS and *Pparγ* was increased with 1.25 and 5% PFHxS. *Pparγ* gene expression increase correlates with the histology data (hepatocellular hypertrophy) and gene expression data (*Cd36*, *Lpl*) as Pparγ is involved in steatosis and development of a fatty liver (Inoue et al., 2005; Matsusue et al., 2003). PPARγ overexpression was also shown to decrease cholesterol in a human liver cell line (Han et al., 2019). *Pparγ* gene expression also increased with oral exposure in mice (Das et al., 2017), similar to that seen with dermal exposure. An increase in liver weight was observed in mice exposed to K^+PFHxS with the data indicating that this increase was due to both PPARα and pregnane X receptor (PXR) activation (Bijland et al., 2011). Mice exposed to PFHxS for one week via oral gavage regulated only a small proportion of Pparα-dependent genes and the greatest percentage of Pparα-independent genes (compared to PFOS, PFOA, and PFNA) (Rosen et al., 2017). These data support PFHxS induced liver toxicity could be occurring from PPAR isoforms and/or other receptors such as PXR.

Based on previous findings (Hall et al., 2012; USEPA, 2002) the hepatocellular hypertrophy occurring in the liver after dermal PFHxS exposure would be considered adverse. Hepatocellular hypertrophy is considered adaptive when only minimal to slight severity is occurring, no necrosis is present, and there are no changes in liver enzyme activity. The hypertrophy occurring in the present study was observed to be “marked” with all 5 mice at all PFHxS exposure concentrations. Necrosis was also observed with all 5 mice at all PFHxS concentrations. Further support of necrosis occurring is the increased *Serpine1* gene expression. The hallmark liver associated enzymes, ALKP and ALT, are also significantly increased with PFHxS exposure. As stated in the USEPA Office of Pesticide Program Guidance Document on Hepatocellular Hypertrophy (USEPA, 2002) “increases should not be considered adverse until they are at least 2-fold–3-fold greater than control levels.” ALT increased 3.66-, 2.9-, and 4.6-fold with 1.25%, 2.5%, and 5% PFHxS, respectively. The USEPA also notes that alkaline phosphatase is a more sensitive indicator, and a 2-fold increase may suggest severe toxicity. In this study ALKP was increased 2.11- and 2.61-fold with 2.5% and 5% PFHxS. All these data suggest that the dermal PFHxS exposure induced adverse histopathology changes in the liver.

Interestingly, no histopathological changes were observed in the skin with PFHxS exposure. This is a difference from the carboxylic acid PFAS previously investigated in our lab where hyperplasia, hyperkeratosis, necrosis, inflammation, and fibrosis were observed with dermal exposure (Weatherly et al., 2021, 2023). Also, skin irritation was observed at the site of application with carboxylic acid PFAS (Weatherly et al., 2023), but no skin irritation was seen with PFHxS exposure. However, even though histopathological changes were not observed, changes in phenotyping of several cell sub-groups ($CD4^+$ and $CD8^+$ T-cells, neutrophils, eosinophils, and $CD11b^+$ DCs) and molecular changes in gene expression (*Il-6, Tslp, Cxcl1, S100a8, Pparγ, Pparδ*) were observed in the skin with PFHxS exposure. These local dermal findings (increase in eosinophils, neutrophils, and *Il-6* gene expression) suggest an inflammatory response at the site of application. The increase in eosinophils could also be significant to previously reported associations between PFHxS and asthma in humans (discussed below). Also, increased gene expression in skin barrier genes *Lor* (2.5 and 5%) and *Flg* (5%) were seen after dermal PFHxS exposure. Interestingly, even with the

lack of histopathology changes in the skin, *Lor* and *Flg* were both increased to a similar level after PFHxS as with PFPeA, PFHxA, and PFHpA (Weatherly et al., 2023). However, PFHxS induced a slight but significant increase in *Pparδ* with 5% PFHxS that was not seen with the carboxylic acid PFAS. Also, the carboxylic acid PFAS induced a decrease in *Pparγ* with multiple concentrations where PFHxS only showed a decrease with the highest concentration. These data suggest possible different mechanisms of dermal toxicity between the different classes of PFAS.

Histopathology data did show decreased lymphocyte cellularity in the spleen and decreased incidence of mononuclear infiltrates in the liver and kidney, consistent with an effect of PFHxS on lymphocytes and the monocytic lineage. This could be due to PFHxS causing cells to migrate out of these tissues or the cells dying due to toxicity. Skin phenotyping revealed an increase in both $CD4^+$ and $CD8^+$ T-cells and dendritic cells with PFHxS exposure along with an increase in $CD8^+$ T cell frequency and DC frequency in the dLN. Additionally, necrosis was also noted in the liver histopathology and *serpine1* (involved in necrosis) was increased in the spleen. These data suggest PFHxS is inducing a combination of both cell migration and toxicity on the lymphocytes and monocytic lineage. None of the previously examined carboxylic acid PFAS showed an effect on spleen, kidney, or liver cellularity (Weatherly et al., 2021, 2023).

Very few animal studies have evaluated the immunotoxicity effects of PFHxS and only one very recent study was found on PFHxS effects on spleen IgM response to SRBC. The SRBC PFC assay requires the cooperation of both B and T-lymphocytes along with macrophages and measures the production of antigen-specific antibodies (IgM isotype). It is the primary murine assay to evaluate humoral immune function and is considered one of the most sensitive assays to assess immunomodulation. Deer mice exposed to PFHxS via oral gavage for 28-days showed a reduction in PFC formation at 7 and 14 mg/kg/d (Narizzano et al., 2023). The current study shows similar results with dermal PFHxS exposure at similar (slightly higher) concentrations. Our lab previously investigated dermal PFOA exposure on immune response and saw PFOA induced suppression of the IgM response to SRBC (Shane et al., 2020). PFOA has also been shown to reduce SRBC IgM antibody titers in mice after 15 days of exposure to 3.75–30 mg/kg PFOA via drinking water (Dewitt et al., 2008). PFOS also reduces SRBC specific IgM response in C57BL/6 mice after 60 days of oral gavage exposure at concentrations from ~0.0834 to 2.1 mg/kg/day (Dong et al., 2009). The decrease in formation of PFC in this study suggests PFHxS induces functional deficits in adaptive immune response.

PFHxS induced a significant decrease in spleen weight with all three concentrations tested and thymus weight was significantly decreased with 2.5 and 5% PFHxS. Also, spleen phenotyping after PFHxS exposure showed a decrease in total cellularity and in both B-cell number and frequency. These data support the immunotoxicity effects demonstrated with the SRBC assay. None of the previously examined carboxylic acid PFAS decreased spleen and/or thymus weight and only PFHpA decreased B-cell frequency and only at the 5% exposure (Weatherly et al., 2021, 2023). The spleen gene expression data also supports immunosuppression occurring after dermal PFHxS exposure. Several genes that are reflective of suppression were altered in the spleen. Sustained TLR7 activation in

mice was suggested to account for the changes in spleen morphology and a decreased antigen-specific humoral immune response (Baenziger et al., 2009). IL-10 has been shown to enable apoptosis of B-cells activated with *Staphylococcus aureus* and lead to a decrease in IgM production (Itoh and Hirohata, 1995) along with controlling the suppression of antigen-specific immunity (Akdis and Blaser, 2001).

Epidemiology studies exist evaluating PFAS exposure and immune suppression and hypersensitivity. Several studies have associated reduced humoral immune response and decreased antibody response to immunizations in childhood with PFAS exposure (von Holst et al., 2021). An increase in PFHxS concentration was associated with a decrease in tetanus antibody levels in 5- and 7-year-old children (Grandjean et al., 2012; Mogensen et al., 2015). An increase in PFHxS levels was also associated with a decrease in rubella antibody titers in seropositive adolescents, however, there was no association for measles or mumps antibody titers (Stein et al., 2016). Another study found increasing odds of asthma with an increase in serum PFHxS in Taiwanese children (Dong et al., 2013; Qin et al., 2017). Elevated serum PFHxS levels were also found in adolescents with asthma (Zhu et al., 2016). However, additional studies are needed to confirm PFHxS effects on human immune suppression and hypersensitivity.

It is important to note that mice were group housed to reduce the potential for unnecessary stress which can influence immune function. As such, there is the potential for PFAS exposure due to grooming, through the drinking water and food source, and tail marking for animal identification. However, these contributions are expected to be minimal and normalized relative to PFHxS exposure since all groups were exposed. It is important to note that these studies were conducted for hazard identification purposes and to confirm dermal absorption of PFHxS through serum and urine analysis. Therefore, the highest non- toxic concentrations were selected for evaluation following dermal exposure. Exposure and risk assessment were beyond the scope of these studies and therefore not assessed. Although the levels detected in the serum were higher than those found in humans, the PFHxS exposure concentrations are comparable to other oral exposure experimental animal studies (Bijland et al., 2011; Das et al., 2017; Narizzano et al. 2021, 2023). There is no data on human serum or urine concentrations after PFHxS occupational or consumer product exposure only occurring dermally and it should be noted that comparisons between species are difficult as PFAS are excreted at different rates in different species (ATSDR, 2021). However, PFAS levels, in general, have been shown to be higher in occupational cohorts compared to the general public (Sonnenberg et al., 2023). Also, human exposures are frequently chronic as opposed to a 28-day exposure with mice and it is possible that in epidemiology studies the peak levels in the serum/urine could be being missed.

In summary, these studies are the first to evaluate the immunotoxicity induced by dermal exposure to PFHxS using a murine model. Significant increases in PFHxS detected in serum and urine along with changes in histology, organ weights, serum chemistries, gene expression, and SRBC IgM response support that PFHxS can be absorbed via the skin and lead to systemic effects and immune suppression. While similar results were observed to dermally exposed carboxylic acid PFAS studies, unique mechanisms of toxicity are suggested between PFHxS and carboxylic acid PFAS. Further investigation into PFAS

dermal exposure is needed to understand the hazards of skin exposure on systemic toxicity and immune function.

Supplementary Material

Refer to Web version on PubMed Central for supplementary material.

Funding information

This work was supported by intramural funds from the National Occupational Research Agenda (NORA) CAN 9390HTP.

Data availability

All study data will be made available on the NIOSH Data and Statistics Gateway.

References

Akdis CA, Blaser K, 2001. Mechanisms of interleukin-10-mediated immune suppression. Immunology 103 (2), 131–136. [PubMed: 11412299]

Andersen ME, Butenhoff JL, Chang SC, Farrar DG, Kennedy GL Jr., Lau C, Olsen GW, Seed J, Wallace KB, 2008. Perfluoroalkyl acids and related chemistries–toxicokinetics and modes of action. Toxicol. Sci 102 (1), 3–14. [PubMed: 18003598]

ATSDR, 2021. Toxicological Profile for Perfluoroalkyls. https://wwwn.cdc.gov/TSP/ToxProfiles/ToxProfiles.aspx?id=1117&tid=237.

Averina M, Brox J, Huber S, Furberg AS, Sørensen M, 2019. Serum perfluoroalkyl substances (pfas) and risk of asthma and various allergies in adolescents. The tromsø study fit futures in northern Norway. Environ. Res 169, 114–121. [PubMed: 30447498]

Baenziger S, Heikenwalder M, Johansen P, Schlaepfer E, Hofer U, Miller RC, Diemand S, Honda K, Kundig TM, Aguzzi A, Speck RF, 2009. Triggering tlr7 in mice induces immune activation and lymphoid system disruption, resembling hiv- mediated pathology. Blood 113 (2), 377–388. [PubMed: 18824599]

Bijland S, Rensen PC, Pieterman EJ, Maas AC, van der Hoorn JW, van Erk MJ, Havekes LM, Willems van Dijk K, Chang SC, Ehresman DJ, et al. , 2011. Perfluoroalkyl sulfonates cause alkyl chain length-dependent hepatic steatosis and hypolipidemia mainly by impairing lipoprotein production in apoe*3-leiden cetp mice. Toxicol. Sci 123 (1), 290–303. [PubMed: 21705711]

Bjork JA, Wallace KB, 2009. Structure-activity relationships and human relevance for perfluoroalkyl acid-induced transcriptional activation of peroxisome proliferation in liver cell cultures. Toxicol. Sci 111 (1), 89–99. [PubMed: 19407336]

Blake BE, Pinney SM, Hines EP, Fenton SE, Ferguson KK, 2018. Associations between longitudinal serum perfluoroalkyl substance (pfas) levels and measures of thyroid hormone, kidney function, and body mass index in the fernald community cohort. Environ. Pollut 242 (Pt A), 894–904. [PubMed: 30373035]

Burgess JL, Fisher JM, Nematollahi A, Jung AM, Calkins MM, Graber JM, Grant CC, Beitel SC, Littau SR, Gulotta JJ, et al. , 2023. Serum per- and polyfluoroalkyl substance concentrations in four municipal us fire departments. Am. J. Ind. Med 66 (5), 411–423. [PubMed: 35864570]

Buser MC, Scinicariello F, 2016. Perfluoroalkyl substances and food allergies in adolescents. Environ. Int 88, 74–79. [PubMed: 26722671]

Butenhoff JL, Chang SC, Ehresman DJ, York RG, 2009. Evaluation of potential reproductive and developmental toxicity of potassium perfluorohexanesulfonate in sprague dawley rats. Reprod. Toxicol 27 (3–4), 331–341. [PubMed: 19429404]

C8 science panel. [accessed]. http://www.c8sciencepanel.org/publications.html.

Calafat AM, Wong LY, Kuklenyik Z, Reidy JA, Needham LL, 2007. Polyfluoroalkyl chemicals in the u.S. Population: data from the national health and nutrition examination survey (nhanes) 2003–2004 and comparisons with nhanes 1999–2000. Environ. Health Perspect 115 (11), 1596–1602. [PubMed: 18007991]

Chang S, Butenhoff JL, Parker GA, Coder PS, Zitzow JD, Krisko RM, Bjork JA, Wallace KB, Seed JG, 2018. Reproductive and developmental toxicity of potassium perfluorohexanesulfonate in cd-1 mice. Reprod. Toxicol 78, 150–168. [PubMed: 29694846]

Costello E, Rock S, Stratakis N, Eckel SP, Walker DI, Valvi D, Cserbik D, Jenkins T, Xanthakos SA, Kohli R, et al. , 2022. Exposure to per- and polyfluoroalkyl substances and markers of liver injury: a systematic review and meta-analysis. Environ. Health Perspect 130 (4), 46001. [PubMed: 35475652]

Crissman JW, Goodman DG, Hildebrandt PK, Maronpot RR, Prater DA, Riley JH, Seaman WJ, Thake DC, 2004. Best practices guideline: Toxicologic histopathology. Toxicol. Pathol 32 (1), 126–131. [PubMed: 14713558]

Das KP, Wood CR, Lin MT, Starkov AA, Lau C, Wallace KB, Corton JC, Abbott BD, 2017. Perfluoroalkyl acids-induced liver steatosis: effects on genes controlling lipid homeostasis. Toxicology 378, 37–52. [PubMed: 28049043]

De Guise S, Levin M, 2021. Suppression of th2 cytokines as a potential mechanism for reduced antibody response following pfoa exposure in female b6c3f1 mice. Toxicol. Lett 351, 155–162. [PubMed: 34517056]

Dewitt JC, Copeland CB, Strynar MJ, Luebke RW, 2008. Perfluorooctanoic acid- induced immunomodulation in adult c57bl/6j or c57bl/6n female mice. Environ. Health Perspect 116 (5), 644–650. [PubMed: 18470313]

DeWitt JC, Williams WC, Creech NJ, Luebke RW, 2016. Suppression of antigen- specific antibody responses in mice exposed to perfluorooctanoic acid: role of pparα and t- and b-cell targeting. J. Immunot 13 (1), 38–45.

Dong GH, Zhang YH, Zheng L, Liu W, Jin YH, He QC, 2009. Chronic effects of perfluorooctanesulfonate exposure on immunotoxicity in adult male c57bl/6 mice. Arch. Toxicol 83 (9), 805–815. [PubMed: 19343326]

Dong GH, Tung KY, Tsai CH, Liu MM, Wang D, Liu W, Jin YH, Hsieh WS, Lee YL, Chen PC, 2013. Serum polyfluoroalkyl concentrations, asthma outcomes, and immunological markers in a case-control study of taiwanese children. Environ. Health Perspect 121 (4), 507–513. [PubMed: 23309686]

Fisher M, Arbuckle TE, Wade M, Haines DA, 2013. Do perfluoroalkyl substances affect metabolic function and plasma lipids?–analysis of the 2007–2009, canadian health measures survey (chms) cycle 1. Environ. Res 121, 95–103. [PubMed: 23266098]

Franko J, Meade BJ, Frasch HF, Barbero AM, Anderson SE, 2012. Dermal penetration potential of perfluorooctanoic acid (pfoa) in human and mouse skin. J. Toxicol. Environ. Health 75 (1), 50–62.

Freberg BI, Haug LS, Olsen R, Daae HL, Hersson M, Thomsen C, Thorud S, Becher G, Molander P, Ellingsen DG, 2010. Occupational exposure to airborne perfluorinated compounds during professional ski waxing. Environ. Sci. Technol 44 (19), 7723–7728. [PubMed: 20831156]

Grandjean P, Andersen EW, Budtz-Jørgensen E, Nielsen F, Mølbak K, Weihe P, Heilmann C, 2012. Serum vaccine antibody concentrations in children exposed to perfluorinated compounds. JAMA 307 (4), 391–397. [PubMed: 22274686]

Hall AP, Elcombe CR, Foster JR, Harada T, Kaufmann W, Knippel A, Küttler K, Malarkey DE, Maronpot RR, Nishikawa A, et al. , 2012. Liver hypertrophy: a review of adaptive (adverse and non-adverse) changes–conclusions from the 3rd international estp expert workshop. Toxicol. Pathol 40 (7), 971–994. [PubMed: 22723046]

Han T, Lv Y, Wang S, Hu T, Hong H, Fu Z, 2019. Pparγ overexpression regulates cholesterol metabolism in human l02 hepatocytes. J. Pharmacol. Sci 139 (1), 1–8. [PubMed: 30554802]

Han JS, Jang S, Son HY, Kim YB, Kim Y, Noh JH, Kim MJ, Lee BS, 2020. Subacute dermal toxicity of perfluoroalkyl carboxylic acids: comparison with different carbon-chain lengths in human skin equivalents and systemic effects of perfluoroheptanoic acid in sprague dawley rats. Arch. Toxicol 94 (2), 523–539. [PubMed: 31797001]

Inoue M, Ohtake T, Motomura W, Takahashi N, Hosoki Y, Miyoshi S, Suzuki Y, Saito H, Kohgo Y, Okumura T, 2005. Increased expression of ppargamma in high fat diet-induced liver steatosis in mice. Biochem. Biophys. Res. Commun 336 (1), 215–222. [PubMed: 16125673]

Itoh K, Hirohata S, 1995. The role of il-10 in human b cell activation, proliferation, and differentiation. J. Immunol 154 (9), 4341–4350. [PubMed: 7722292]

Jerne NK, Nordin AA, 1963. Plaque formation in agar by single antibody-producing cells. Science 140 (3565), 405.

Jin C, Sun Y, Islam A, Qian Y, Ducatman A, 2011. Perfluoroalkyl acids including perfluorooctane sulfonate and perfluorohexane sulfonate in firefighters. J. Occup. Environ. Med 53 (3), 324–328. [PubMed: 21346631]

Kersten S, 2008. Peroxisome proliferator activated receptors and lipoprotein metabolism. PPAR Res, 132960, 2008.

Khalil N, Ducatman AM, Sinari S, Billheimer D, Hu C, Littau S, Burgess JL, 2020. Per- and polyfluoroalkyl substance and cardio metabolic markers in firefighters. J. Occup. Environ. Med 62 (12), 1076–1081. [PubMed: 33105404]

Kotthoff M, Müller J, Jürling H, Schlummer M, Fiedler D, 2015. Perfluoroalkyl and polyfluoroalkyl substances in consumer products. Environ. Sci. Pollut. Res. Int 22 (19), 14546–14559. [PubMed: 25854201]

Laitinen JA, Koponen J, Koikkalainen J, Kiviranta H, 2014. Firefighters' exposure to perfluoroalkyl acids and 2-butoxyethanol present in firefighting foams. Toxicol. Lett 231 (2), 227–232. [PubMed: 25447453]

Lau C, Anitole K, Hodes C, Lai D, Pfahles-Hutchens A, Seed J, 2007. Perfluoroalkyl acids: a review of monitoring and toxicological findings. Toxicol. Sci 99 (2), 366–394. [PubMed: 17519394]

Lindstrom AB, Strynar MJ, Libelo EL, 2011. Polyfluorinated compounds: past, present, and future. Environ. Sci. Technol 45 (19), 7954–7961. [PubMed: 21866930]

Maizel A, Thompson A, Tighe M, Escobar S, Rodowa A, Falkenstein-Smith R, Benner B Jr., Hoffman K, Donnelly M, Hernandez O, et al. , 2023. Per- and Polyfluroalkyl Substances in New Firefighter Turnout Gear Textiles. NIST Technical Note 2248.

Matsusue K, Haluzik M, Lambert G, Yim SH, Gavrilova O, Ward JM, Brewer B Jr., Reitman ML, Gonzalez FJ, 2003. Liver-specific disruption of ppargamma in leptin-deficient mice improves fatty liver but aggravates diabetic phenotypes. J. Clin. Invest 111 (5), 737–747. [PubMed: 12618528]

Mogensen UB, Grandjean P, Heilmann C, Nielsen F, Weihe P, Budtz-Jørgensen E, 2015. Structural equation modeling of immunotoxicity associated with exposure to perfluorinated alkylates. Environ. Health 14, 47. [PubMed: 26041029]

Narizzano AM, Bohannon ME, East AG, McDonough C, Choyke S, Higgins CP, Quinn MJ Jr., 2021. Patterns in serum toxicokinetics in peromyscus exposed to per- and polyfluoroalkyl substances. Environ. Toxicol. Chem 40 (10), 2886–2898. [PubMed: 34236102]

Narizzano AM, Bohannon ME, East AG, Guigni BA, Quinn MJ Jr., 2023. Reproductive and immune effects emerge at similar thresholds of pfhxs in deer mice. Reprod. Toxicol 120, 108421.

Nelson JW, Hatch EE, Webster TF, 2010. Exposure to polyfluoroalkyl chemicals and cholesterol, body weight, and insulin resistance in the general u.S. Population. Environ. Health Perspect 118 (2), 197–202. [PubMed: 20123614]

Peaslee GF, Wilkinson JT, McGuinness SR, Tighe M, Caterisano N, Lee S, Gonzales A, Roddy M, Mills S, Mitchell K, 2020. Another pathway for firefighter exposure to per- and polyfluoroalkyl substances: firefighter textiles. Environ. Sci. Technol. Lett 7 (8), 594–599.

Peters JM, Hennuyer N, Staels B, Fruchart JC, Fievet C, Gonzalez FJ, Auwerx J, 1997. Alterations in lipoprotein metabolism in peroxisome proliferator- activated receptor alpha-deficient mice. J. Biol. Chem 272 (43), 27307–27312. [PubMed: 9341179]

Plassmann MM, Berger U, 2013. Perfluoroalkyl carboxylic acids with up to 22 carbon atoms in snow and soil samples from a ski area. Chemosphere 91 (6), 832–837. [PubMed: 23466094]

Poothong S, Thomsen C, Padilla-Sanchez JA, Papadopoulou E, Haug LS, 2017. Distribution of novel and well-known poly- and perfluoroalkyl substances (pfass) in human serum, plasma, and whole blood. Environ. Sci. Technol 51 (22), 13388–13396. [PubMed: 29056041]

Qin XD, Qian ZM, Dharmage SC, Perret J, Geiger SD, Rigdon SE, Howard S, Zeng XW, Hu LW, Yang BY, et al. , 2017. Association of perfluoroalkyl substances exposure with impaired lung function in children. Environ. Res 155, 15–21. [PubMed: 28171771]

Ragnarsdóttir O, Abdallah MA, Harrad S, 2022. Dermal uptake: an important pathway of human exposure to perfluoroalkyl substances? Environ. Pollut 307, 119478.

Rakhshandehroo M, Knoch B, Müller M, Kersten S, 2010. Peroxisome proliferator- activated receptor alpha target genes. PPAR Res. 2010, 612089.

Rosen MB, Das KP, Rooney J, Abbott B, Lau C, Corton JC, 2017. Pparα- independent transcriptional targets of perfluoroalkyl acids revealed by transcript profiling. Toxicology 387, 95–107. [PubMed: 28558994]

Rosenfeld PE, Spaeth KR, Remy LL, Byers V, Muerth SA, Hallman RC, Summers-Evans J, Barker S, 2023. Perfluoroalkyl substances exposure in firefighters: sources and implications. Environ. Res 220, 115164.

Shane HL, Baur R, Lukomska E, Weatherly L, Anderson SE, 2020. Immunotoxicity and allergenic potential induced by topical application of perfluorooctanoic acid (pfoa) in a murine model. Food Chem. Toxicol 136, 111114.

Shoemaker JA, Grimmett P, Boutin B, 2008. Determination of selected perfluorinated alkyl acids in drinking water by solid phase extraction and liquid chromatography/ tandem mass spectrometry (lc/ms/ms. https://cfpub.epa.gov/si/si_public_record_report.cfm?Lab=NERL&dirEntryId=198984&simpleSearch=1&searchAll=EPA%2F600%2FR-08%2F092+.

Sonnenberg NK, Ojewole AE, Ojewole CO, Lucky OP, Kusi J, 2023. Trends in serum per- and polyfluoroalkyl substance (pfas) concentrations in teenagers and adults, 1999–2018 nhanes. Int. J. Environ. Res. Publ. Health 20 (21).

Steenland K, Zhao L, Winquist A, Parks C, 2013. Ulcerative colitis and perfluorooctanoic acid (pfoa) in a highly exposed population of community residents and workers in the mid-Ohio valley. Environ. Health Perspect 121 (8), 900–905. [PubMed: 23735465]

Stein CR, McGovern KJ, Pajak AM, Maglione PJ, Wolff MS, 2016. Perfluoroalkyl and polyfluoroalkyl substances and indicators of immune function in children aged 12–19 y: National health and nutrition examination survey. Pediatr. Res 79 (2), 348–357. [PubMed: 26492286]

Trowbridge J, Gerona RR, Lin T, Rudel RA, Bessonneau V, Buren H, Morello- Frosch R, 2020. Exposure to perfluoroalkyl substances in a cohort of women firefighters and office workers in san francisco. Environ. Sci. Technol 54 (6), 3363–3374. [PubMed: 32100527]

USEPA, 2002. Hepatocellular Hypertrophy file:///C:/Users/nux6/Downloads/625713%20(2).pdf.

USEPA, 2022. Our Current Understanding of the Human Health and Environmental Risks of Pfas. https://www.epa.gov/pfas/our-current-understanding-human-health-and-environmental-risks-pfas#:~:text=People%20Can%20Be%20Exposed%20to%20PFAS%20in%20a%20Variety%20of%20Ways&text=Current%20research%20has%20shown%20that,may%20contain%20PFAS%2C%20including%20fish.

von Holst H, Nayak P, Dembek Z, Buehler S, Echeverria D, Fallacara D, John L, 2021. Perfluoroalkyl substances exposure and immunity, allergic response, infection, and asthma in children: review of epidemiologic studies. Heliyon 7 (10), e08160.

Wang Z, DeWitt JC, Higgins CP, Cousins IT, 2017. A never-ending story of per- and polyfluoroalkyl substances (pfass)? Environ. Sci. Technol 51 (5), 2508–2518. [PubMed: 28224793]

Weatherly LM, Shane HL, Lukomska E, Baur R, Anderson SE, 2021. Systemic toxicity induced by topical application of heptafluorobutyric acid (PFBA) in a murine model. Food Chem. Toxicol 156, 112528.

Weatherly LM, Shane HL, Lukomska E, Baur R, Anderson SE, 2023. Systemic toxicity induced by topical application of perfluoroheptanoic acid (pfhpa), perfluorohexanoic acid (pfhxa), and perfluoropentanoic acid (pfpea) in a murine model. Food Chem. Toxicol 171, 113515.

Whitehead HD, Venier M, Wu Y, Eastman E, Urbanik S, Diamond ML, Shalin A, Schwartz-Narbonne H, Bruton TA, Blum A, et al. , 2021. Fluorinated compounds in north american cosmetics. Environ. Sci. Technol. Lett 8 (7), 538–544.

Wolf CJ, Takacs ML, Schmid JE, Lau C, Abbott BD, 2008. Activation of mouse and human peroxisome proliferator-activated receptor alpha by perfluoroalkyl acids of different functional groups and chain lengths. Toxicol. Sci 106 (1), 162–171. [PubMed: 18713766]

Yang Q, Guo X, Sun P, Chen Y, Zhang W, Gao A, 2018. Association of serum levels of perfluoroalkyl substances (pfass) with the metabolic syndrome (mets) in Chinese male adults: a cross-sectional study. Sci. Total Environ 621, 1542–1549. [PubMed: 29054655]

Young AS, Sparer-Fine EH, Pickard HM, Sunderland EM, Peaslee GF, Allen JG, 2021. Per- and polyfluoroalkyl substances (pfas) and total fluorine in fire station dust. J. Expo. Sci. Environ. Epidemiol 31 (5), 930–942. [PubMed: 33542478]

Zhao L, Teng M, Zhao X, Li Y, Sun J, Zhao W, Ruan Y, Leung KMY, Wu F, 2023. Insight into the binding model of per- and polyfluoroalkyl substances to proteins and membranes. Environ. Int 175, 107951. [PubMed: 37126916]

Zheng L, Dong GH, Jin YH, He QC, 2009. Immunotoxic changes associated with a 7-day oral exposure to perfluorooctanesulfonate (pfos) in adult male c57bl/6 mice. Arch. Toxicol 83 (7), 679–689. [PubMed: 19015834]

Zheng L, Dong GH, Zhang YH, Liang ZF, Jin YH, He QC, 2011. Type 1 and type 2 cytokines imbalance in adult male c57bl/6 mice following a 7-day oral exposure to perfluorooctanesulfonate (pfos). J. Immunot 8 (1), 30–38.

Zhu Y, Qin XD, Zeng XW, Paul G, Morawska L, Su MW, Tsai CH, Wang SQ, Lee YL, Dong GH, 2016. Associations of serum perfluoroalkyl acid levels with thelper cell-specific cytokines in children: by gender and asthma status. Sci. Total Environ 559, 166–173. [PubMed: 27060656]

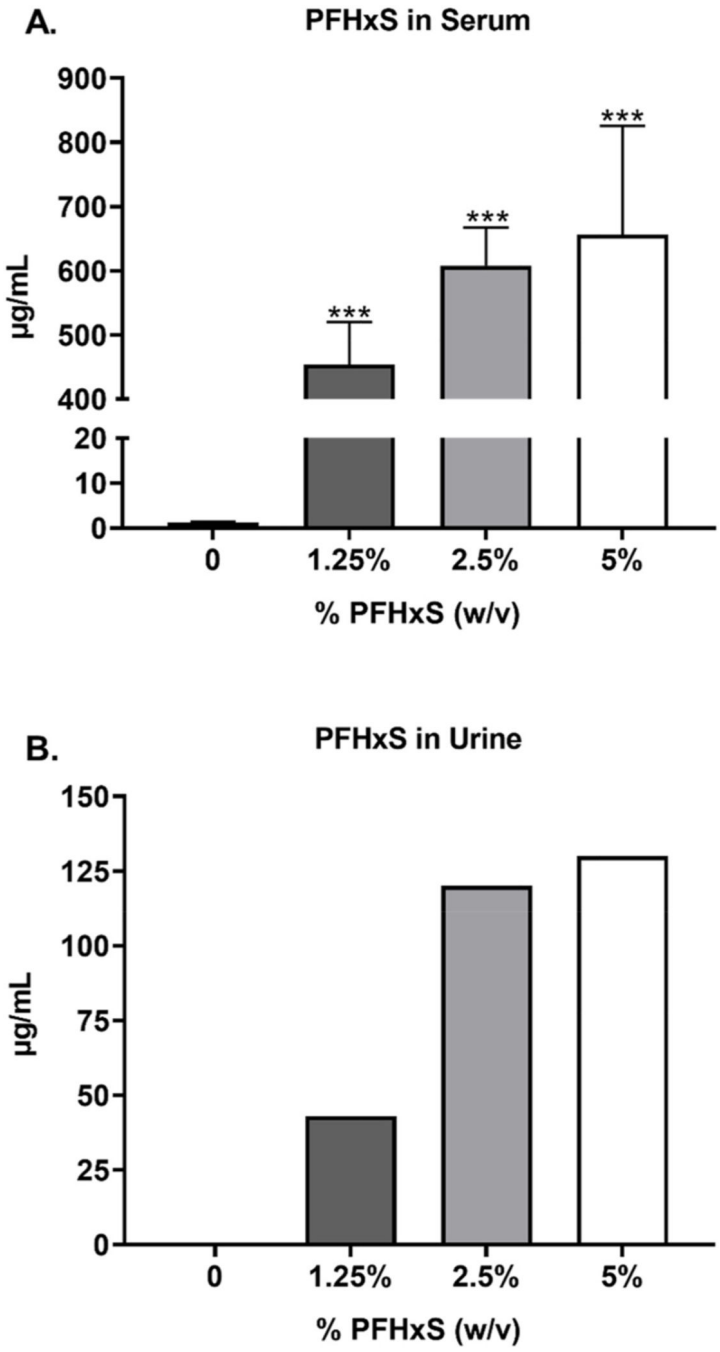

Fig. 1. Changes in PFHxS concentration in serum and urine 24 h after the last dermal exposure.

Analysis of changes in the concentration of PFHxS in serum samples (A) and concentration of PFHxS in urine samples (B) following 28 days of PFHxS exposure. Each concentration represents mean (±SE) of 5 mice per group. Urine concentrations are 5 pooled samples per group. Statistical significance, relative to 0% vehicle control, was determined by one-way ANOVA followed by Dunnett's post-test indicated as ***$p < 0.001$.

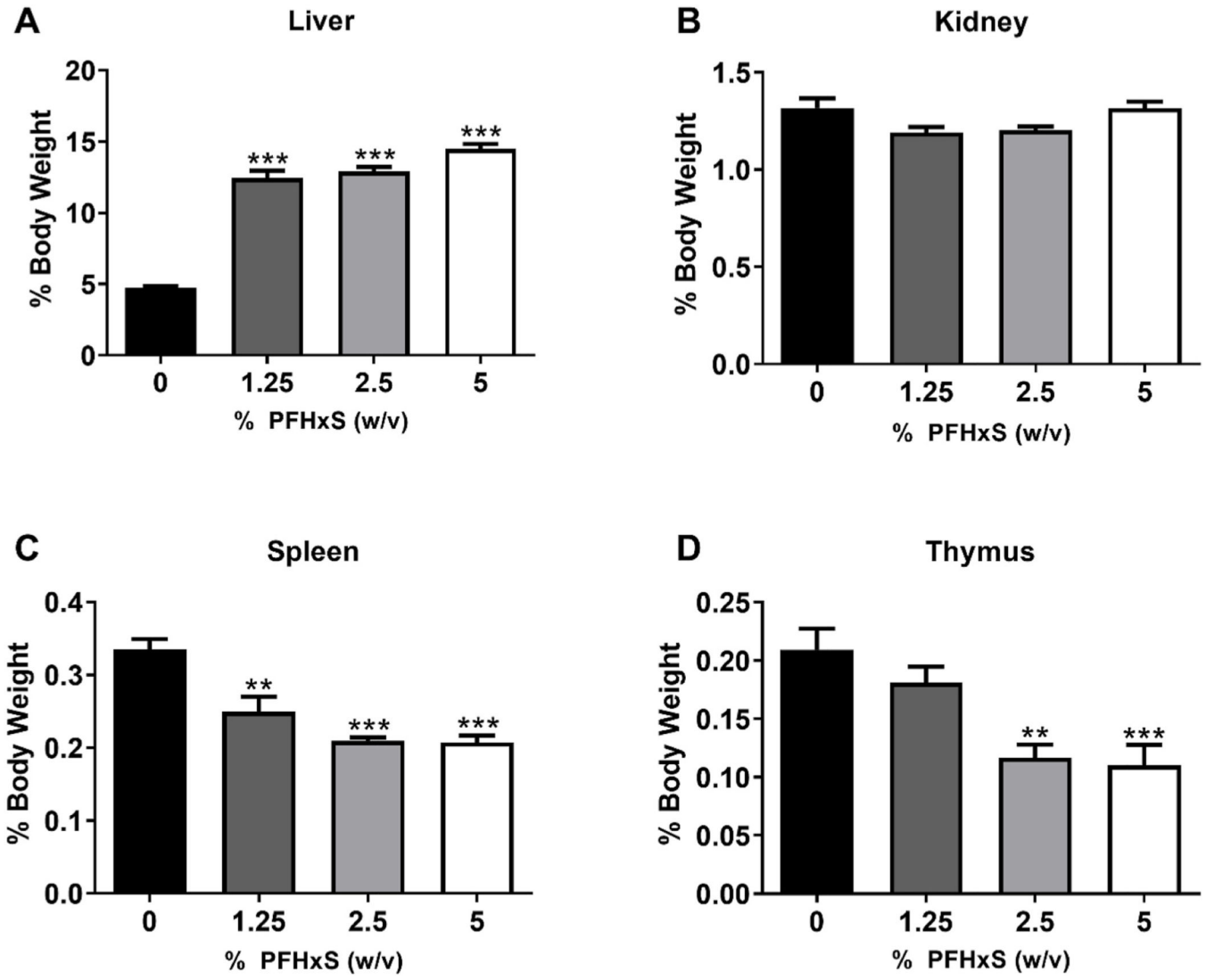

Fig. 2. Changes in organ weights after dermal exposure to PFHxS.

Analysis of changes in liver (A), kidney (B), spleen (C), and thymus (D) weights following 28 days of PFHxS exposure. Data is displayed as organ weight as % body weight. Each concentration represents mean (±SE) of 5 mice per group. Statistical significance, relative to 0% control, was determined by one-way ANOVA followed by Dunnett's post-test indicated as **$p < 0.01$, ***$p < 0.001$.

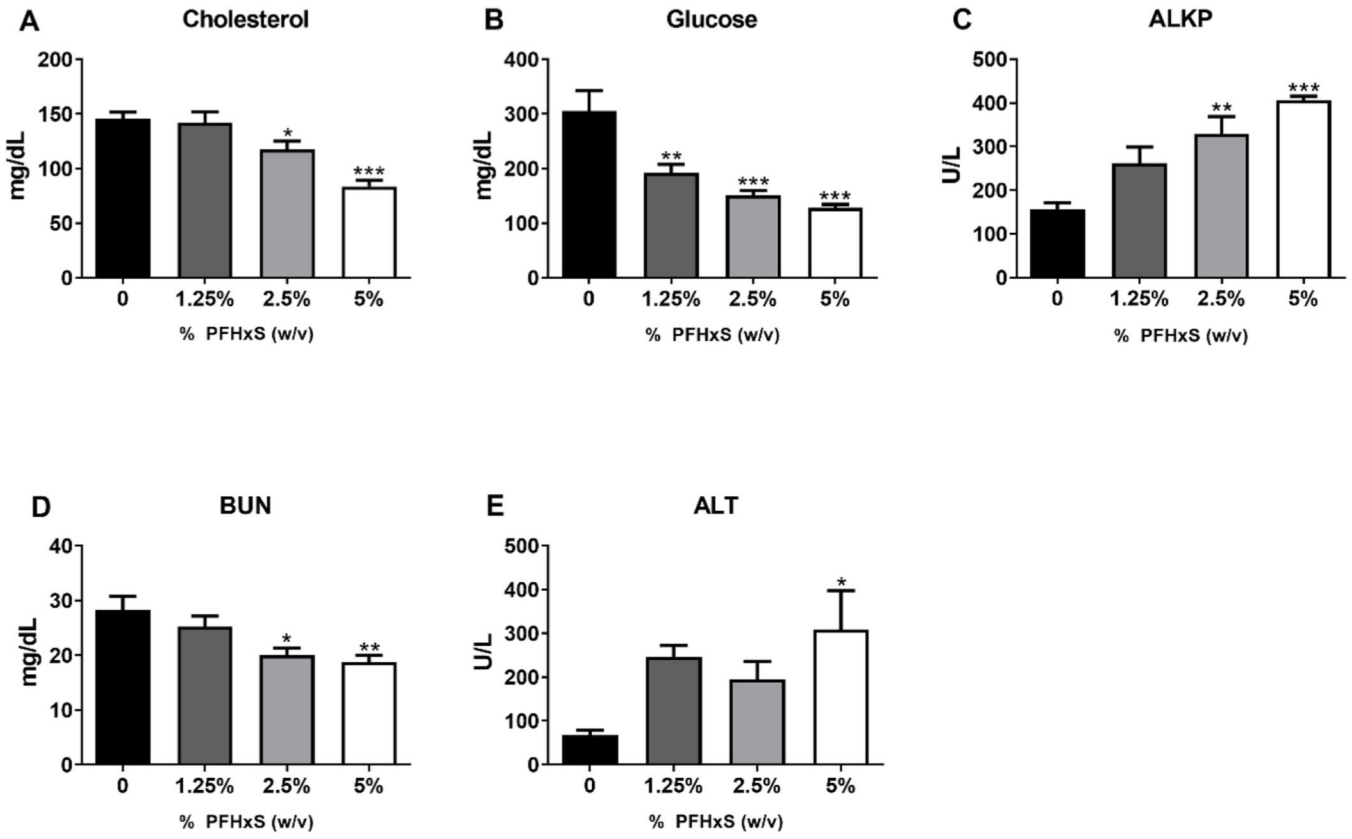

Fig. 3. Changes in serum chemistry after dermal exposure to PFHxS.

Analysis of changes in cholesterol (A), glucose (B), alkaline phosphatase (ALKP) (C), urea nitrogen (D), and alanine aminotransferase (ALT) (E) following 28 days of PFHxS exposure. Each concentration represents mean (±SE) of 4–5 mice per group. Statistical significance, relative to 0% vehicle control, was determined by one-way ANOVA followed by Dunnett's post-test indicated as *$p < 0.05$, **$p < 0.01$, ***$p < 0.001$.

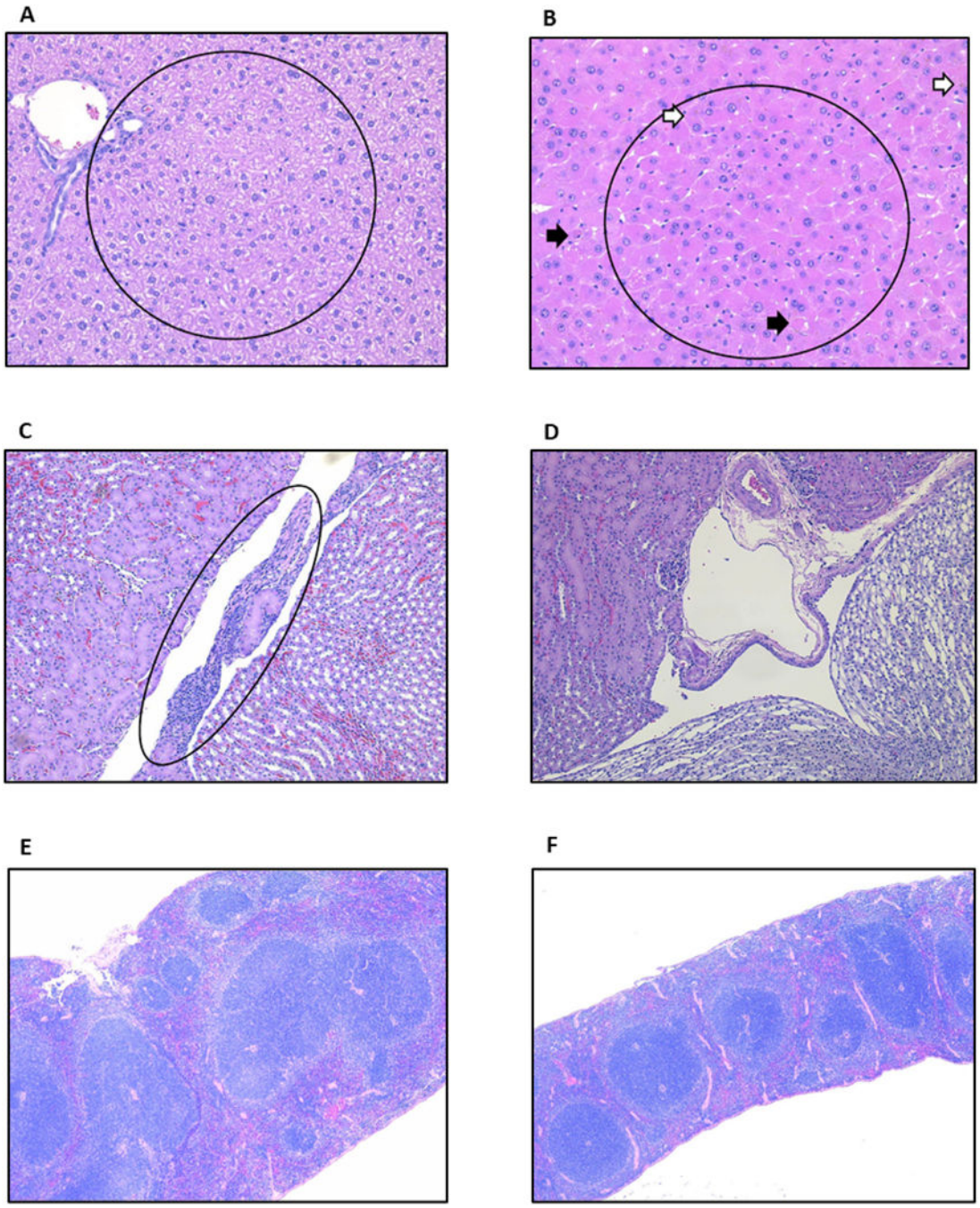

Fig. 4. Histopathology of liver, kidney, and spleen following dermal exposure to PFHxS.

Representative H&E-stained liver, kidney, and spleen sections from control (A, C, and E, respectively) and 5% PFHxS-treated mice (B, D, and F, respectively). (A) Vehicle control 0% PFHxS exposure shows normal liver, note size of hepatocytes and normal cytoplasmic rarefaction (black circle), 20*X* magnification. (B) Marked centrilobular hepatocyte hypertrophy (note size and eosinophilia of hepatocytes (black circle)), minimal necrosis of individual hepatocytes (black arrows), and intracellular pigment consistent with bile (white arrows) was found in 5% PFHxS exposed mice, 20*X* magnification. (C)

Vehicle control 0% PFHxS exposure shows normal kidney with background mononuclear infiltrate (note infiltrate in stroma of renal pelvis (oval)), 10*X* magnification. (D) No mononuclear infiltrates were noted in the renal pelvic interstitium of 5% PFHxS-treated animal, 10*X* magnification. (E) Vehicle control 0% PFHxS exposure shows normal spleen (note overall thickness of spleen and size of lymphoid aggregates), 5*X* magnification. (F) Mildly decreased lymphocytic cellularity, decreased overall thickness of the spleen, and decreased size of lymphoid aggregates were observed with 5% PFHxS exposed mice, 5*X* magnification.

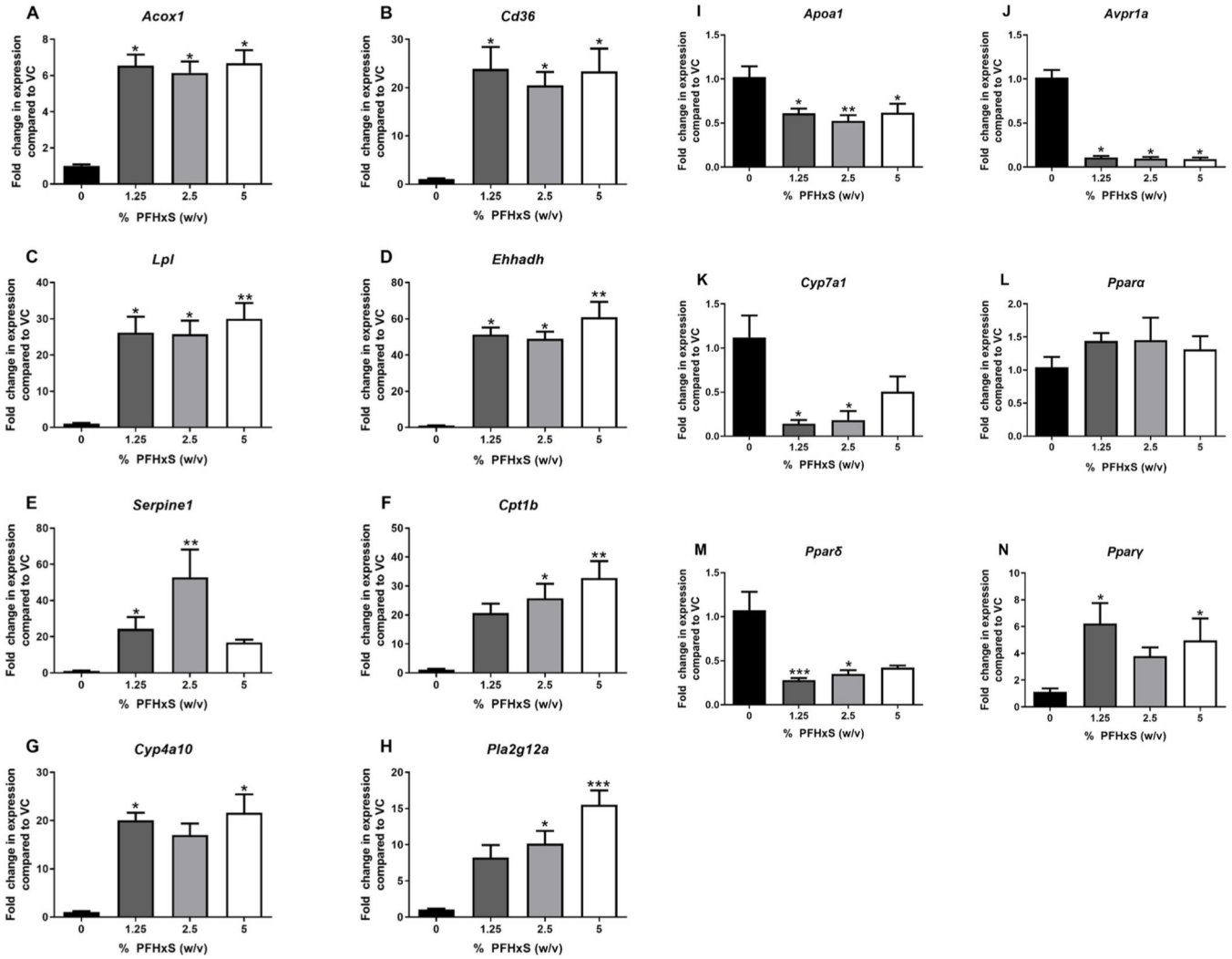

Fig. 5. Liver gene expression following dermal exposure to PFHxS.

Gene expression in the liver following 28 days of PFHxS exposure. Changes in *Acox1* (A), *Cd36* (B), *Lpl* (C), *Ehhadh* (D), *Serpine1* (E), *Cpt1b* (F), *Cyp4a10* (G), *Pla2g12a* (H), *Apoa1* (I), *Avpr1a* (J), *Cyp7a1* (K), *Pparα* (L), *Pparδ* (M), and *Pparγ* (N) were evaluated. Data shown as the mean (±SE) of 4–5 mice per group. Statistical significance, relative to 0% vehicle control (VC), was determined by one-way ANOVA with Dunnett's post-test where *$p < 0.05$, **$p < 0.01$, ***$p < 0.001$. Kruskal-Wallis with Dunn's post-test was conducted for *Acox1, Cd36, Lpl, Ehhadh, Serpine1, Cpt1b, Cyp4a10, Pla2g12a, Avpr1a, Cyp7a1, Pparδ*, and *Pparγ* due to unequal variance.

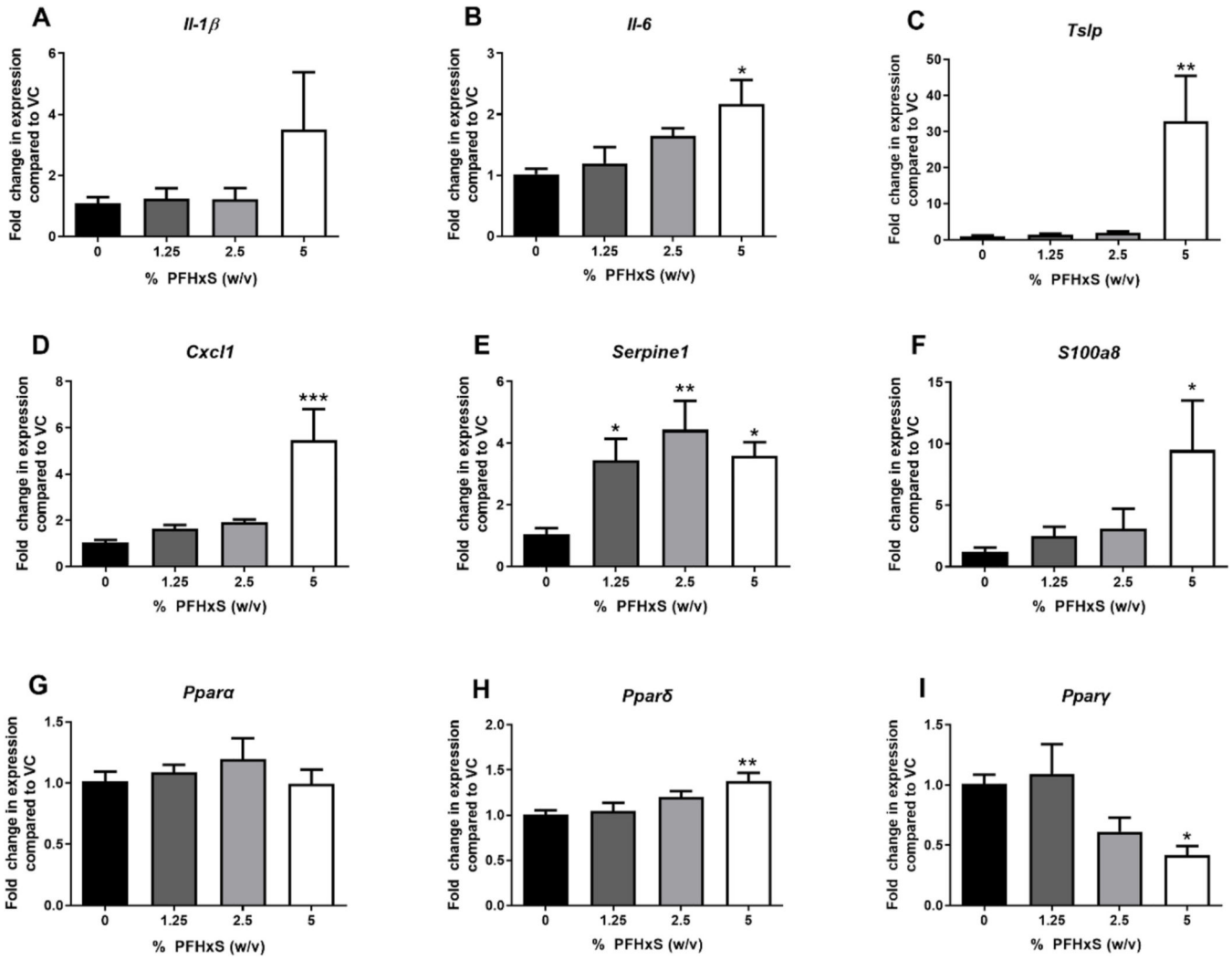

Fig. 6. Skin gene expression following dermal exposure to PFHxS.

Gene expression in the ear following 28 days of PFHxS exposure. Changes in *Il-1β* (A), *Il-6* (B), *Tslp* (C), *Cxcl1* (D), *Serpine1* (E), *S100a8* (F), *Pparα* (G), *Pparδ* (H), and *Pparγ* (I) were evaluated. Data shown as the mean (±SE) of 5 mice per group. Statistical significance, relative to 0% vehicle control (VC), was determined by one-way ANOVA with Dunnett's post-test where *$p < 0.05$, **$p < 0.01$, ***$p < 0.001$. Kruskal- Wallis with Dunn's post-test was conducted for *Il-1β*, *Il-6*, *Tslp*, *Cxcl1*, and *S100a8* due to unequal variance.

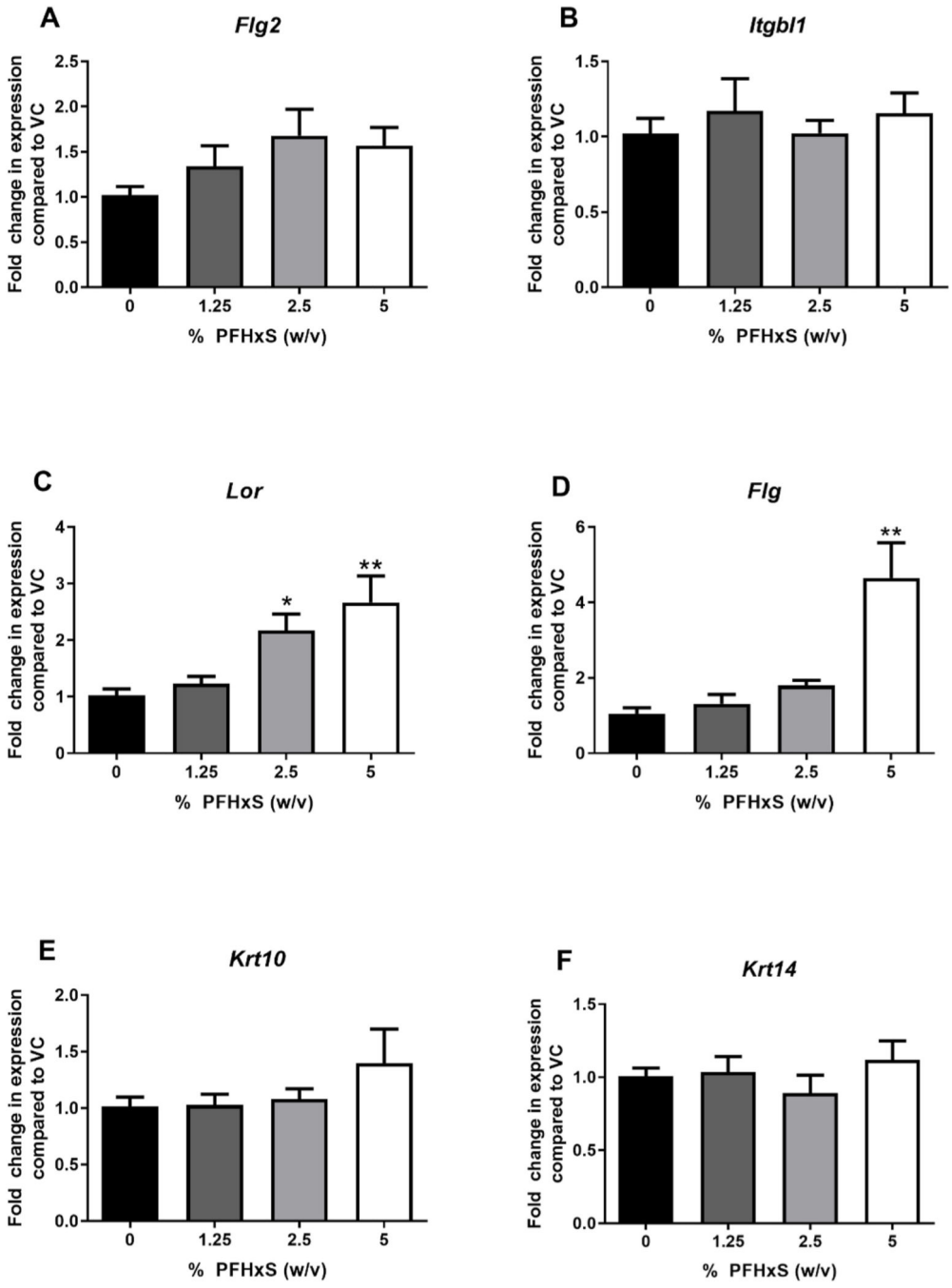

Fig. 7. Skin barrier gene expression following dermal exposure to PFHxS.

Gene expression in the ear following 28 days of PFAS exposure. Changes in *Flg2* (A), *Itgbl1* (B), *Lor* (C), *Flg* (D), *Krt10* (E), and *Krt14* (F) were evaluated. Data shown as the mean (±SE) of 5 mice per group. Statistical significance, relative to 0% vehicle control (VC), was determined by one-way ANOVA with Dunnett's post-test where *$p < 0.05$, **$p < 0.01$. Kruskal-Wallis with Dunn's post-test was conducted for *Lor*, *Flg*, and *Krt10* due to unequal variance.

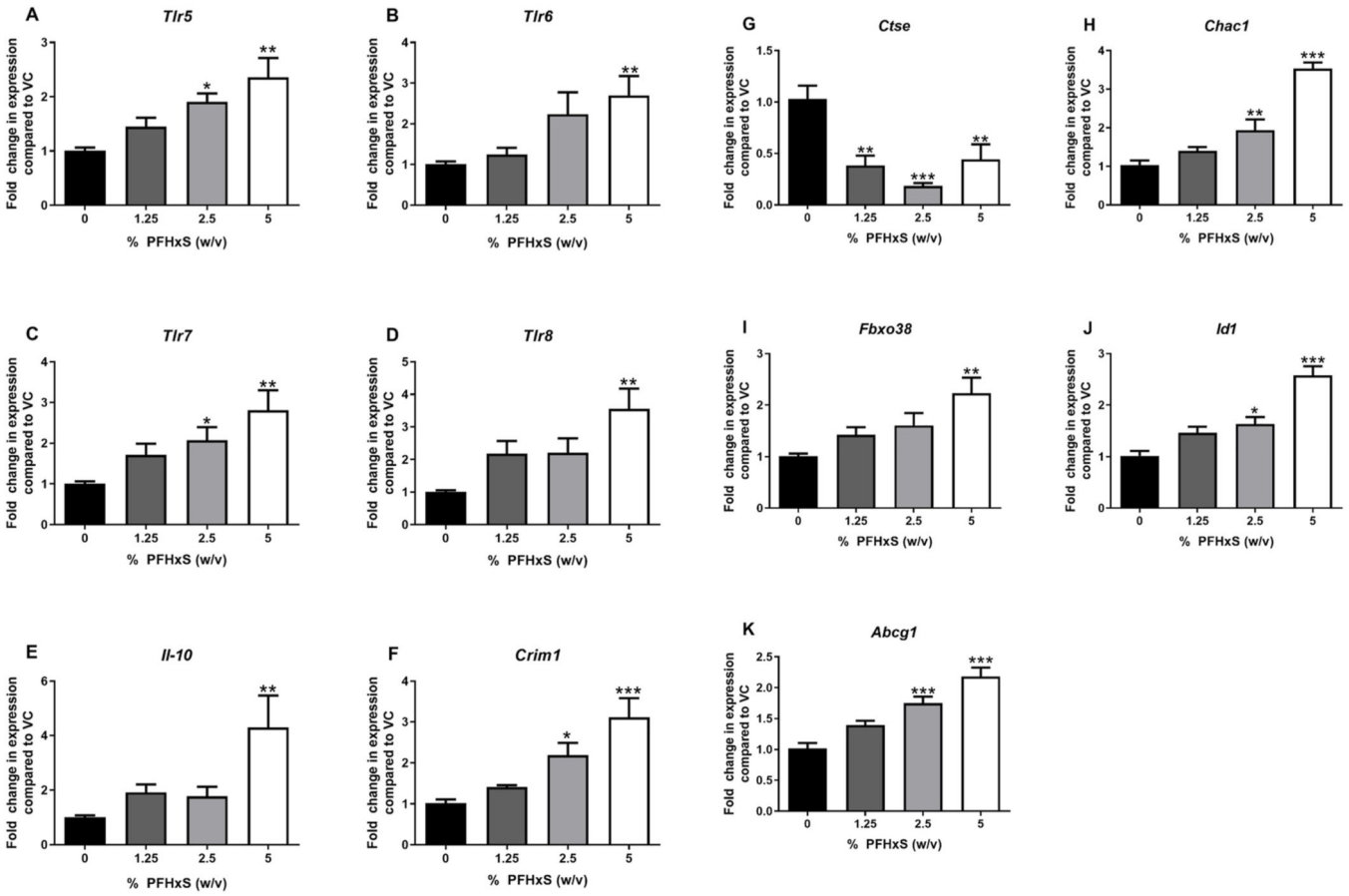

Fig. 8. Spleen gene expression following dermal exposure to PFHxS.

Gene expression in the spleen following 28 days of PFHxS exposure. Changes in *Tlr5* (A), *Tlr6* (B), *Tlr7* (C), *Tlr8* (D), *Il-10* (E), *Crim1* (F), *Ctse* (G), *Chac1* (H), *Fbxo38* (I), *Id1* (J), and *Abcg1* (K) were evaluated. Data shown as the mean (±SE) of 5 mice per group. Statistical significance, relative to 0% vehicle control (VC), was determined by one-way ANOVA with Dunnett's post-test where *$p < 0.05$, **$p < 0.01$, ***$p < 0.001$. Kruskal-Wallis with Dunn's post-test was conducted for *Tlr5*, *Tlr6*, *Tlr7*, *Tlr8*, *Il-10*, *Crim1*, *Ctse* and *Fbxo38* due to unequal variance.

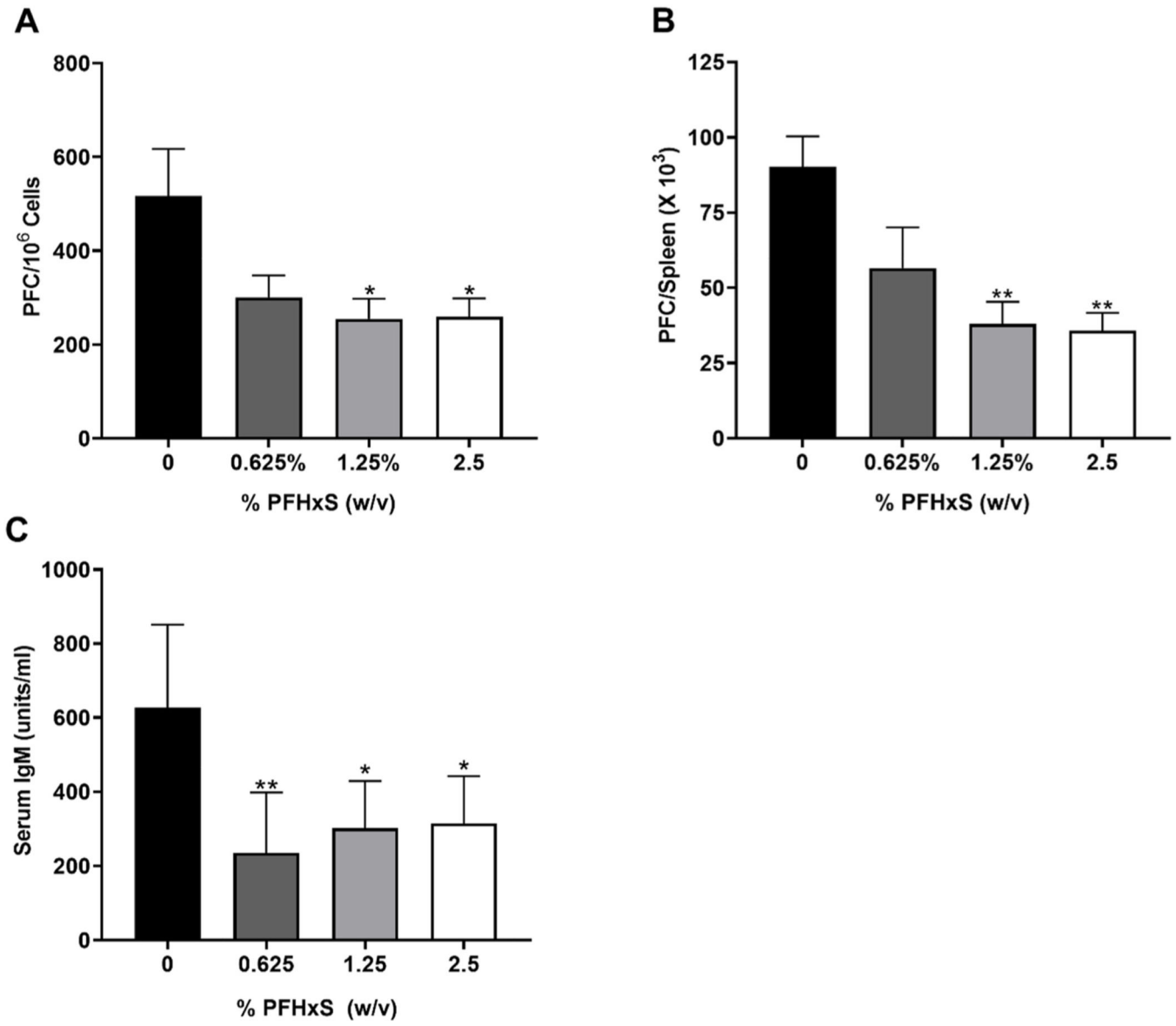

Fig. 9. Dermal PFHxS exposure suppresses the spleen IgM response to SRBC.

Analysis of antibody producing spleen cells after a 10-day dermal exposure to PFHxS suppressed the (A) specific activity, (B) total activity, and (C) serum IgM response to SRBC. Bars represent mean fold-change (±SE) of 4–5 mice per group. Statistical significance, relative to 0% vehicle control, was determined by one-way ANOVA followed by Dunnett's post-test indicated as *$p < 0.05$ and **$p < 0.01$.

Table 1

Incidence and degree of organ injury following dermal exposure to PFHxS in mice.

	28 days			
Parameter	**0%**	**1.25%**	**2.5%**	**5%**
Liver				
Hypertrophy, hepatocyte				
Marked	0	5	5	5
Necrosis				
Minimal	0	3	4	4
Mild	0	2	1	1
Bile, increased, hepatocyte				
Minimal	0	5	5	5
Pigment macrophage				
Minimal	0	4	5	4
Infiltrate, mononucular cell				
Minimal	5	2	2	1
Mild	0	1	0	0
Kidney				
Infiltrate, mononuclear cell				
Minimal	4	0	0	0
Spleen				
Decreased cellularity, lymphocyte				
Mild	0	2	4	5

Table 2

Skin phenotyping of mice dermally exposed to PFHxS.

Skin	**28 days**			
Parameter	**0%**	**1.25%**	**2.5%**	**5%**
Cellularity (x 10^5)	9.85 ± 0.44	9.56 ± 0.21	**7.67 ± 0.62** **	9.56 ± 0.31
$CD45^+$ (x 10^4)	8.03 ± 0.44	8.39 ± 0.66	6.35 ± 0.84	**1.29 ± 0.56** ***
$CD45^+$ (%)	8.14 ± 0.20	8.29 ± 0.74	8.20 ± 0.74	**13.48 ± 0.52** ***
$CD4^+$ (x 10^3)	1.66 ± 0.12	2.31 ± 0.36	2.10 ± 0.25	**5.82 ± 0.41** ***
$CD4^+$ (%)	2.07 ± 0.12	2.64 ± 0.25	**3.34 ± 0.18** ***	**4.51 ± 0.21** ***
$CD8^+$ (x 10^2)	1.29 ± 0.07	3.21 ± 0.60	2.52 ± 0.48	**9.37 ± 1.32** ***
$CD8^+$ (%)	0.16 ± 0.01	0.36 ± 0.05	**0.41 ± 0.07** *	**0.73 ± 0.09** ***
NK (x 10^2)	10.30 ± 1.17	8.53 ± 1.49	**4.86 ± 0.61** **	8.76 ± 0.68
NK (%)	1.27 ± 0.09	0.97 ± 0.11	**0.78 ± 0.07** **	**0.68 ± 0.04** ***
Eosinophils (x 10^3)	1.67 ± 0.12	1.00 ± 0.24	1.10 ± 0.15	**3.49 ± 0.52** **
Eosinophils (%)	2.09 ± 0.16	**1.21 ± 0.20** *	1.75 ± 0.12	2.68 ± 0.31
Neutrophils (x 10^2)	2.58 ± 0.13	1.79 ± 0.31	1.84 ± 0.33	**14.10 ± 4.21** **
Neutrophils (%)	0.32 ± 0.01	0.23 ± 0.03	0.30 ± 0.05	**1.14 ± 0.37** *
CD11b- DCs (x 10^2)	15.30 ± 0.97	12.30 ± 1.74	**7.66 ± 1.11** **	16.10 ± 1.39
CD11b- DCs (%)	1.90 ± 0.07	**1.43 ± 0.18** *	**1.23 ± 0.12** **	**1.25 ± 0.08** **
CD11b + DCs (x 10^2)	6.18 ± 0.73	5.17 ± 0.30	4.45 ± 0.48	**15.10 ± 0.45** ***
CD11b + DCs (%)	0.77 ± 0.08	0.64 ± 0.03	0.73 ± 0.08	**1.18 ± 0.05** ***

Values are expressed as the means (±SE) for each group (n = 4–5 mice/group).

* $p < 0.05$

** $p < 0.01$

*** $p < 0.001$.

Table 3

Spleen phenotyping of mice dermally exposed to PFHxS.

Spleen	28 days			
Parameter	**0%**	**1.25%**	**2.5%**	**5%**
Cellularity (x 10^7)	9.99 ± 1.15	7.91 ± 1.16	**4.99 ± 0.55** **	**3.68 ± 0.45** ***
$CD4^+$ (x 10^7)	2.19 ± 0.24	1.95 ± 0.30	**1.30 ± 0.13** *	**0.99 ± 0.12** **
$CD4^+$ (%)	21.94 ± 0.92	24.60 ± 0.70	**26.26 ± 0.79** **	**26.90 ± 0.70** **
$CD8^+$ (x 10^6)	13.50 ± 1.48	11.70 ± 1.45	**8.25 ± 0.73** *	**6.58 ± 0.73** **
$CD8^+$ (%)	13.58 ± 0.61	15.12 ± 0.73	**16.74 ± 0.56** **	**18.12 ± 0.59** ***
B-cells (x 10^7)	3.48 ± 0.43	2.50 ± 0.38	**1.62 ± 0.19** **	**1.11 ± 0.15** ***
B-cells (%)	34.78 ± 1.62	31.48 ± 0.59	32.48 ± 0.37	**30.06 ± 0.55** **
NK (x 10^5)	29.00 ± 4.26	20.00 ± 3.26	**10.90 ± 1.04** ***	**6.35 ± 0.96** ***
NK (%)	2.87 ± 0.13	2.52 ± 0.17	**2.19 ± 0.06** **	**1.71 ± 0.17** ***
Neutrophils (x 10^5)	15.70 ± 2.34	14.00 ± 2.38	8.87 ± 2.15	9.14 ± 1.54
Neutrophils (%)	1.55 ± 0.08	1.76 ± 0.14	1.69 ± 0.21	**2.51 ± 0.34** *
Dendritic Cells (x 10^6)	2.96 ± 0.33	2.70 ± 0.48	1.71 ± 0.33	**1.26 ± 0.20** **
Dendritic Cells (%)	2.96 ± 0.06	3.33 ± 0.32	3.36 ± 0.48	3.34 ± 0.31
CD11b+ (x 10^6)	4.53 ± 0.60	3.13 ± 0.51	**1.56 ± 0.24** ***	**0.93 ± 0.15** ***
CD11b+ (%)	4.50 ± 0.21	3.90 ± 0.21	**3.07 ± 0.21** ***	**2.49 ± 0.24** ***
CD11b + Ly6C+ (x 10^5)	10.90 ± 1.27	9.05 ± 1.59	**3.77 ± 0.85** **	**2.52 ± 0.56** ***
CD11b + Ly6C+ (%)	1.09 ± 0.03	1.11 ± 0.09	**0.72 ± 0.11** *	**0.68 ± 0.13** *
CD11b + Ly6C- (x 10^5)	32.40 ± 4.53	**21.00 ± 3.46** *	**11.20 ± 1.52** ***	**6.28 ± 0.91** ***
CD11b + Ly6C- (%)	3.22 ± 0.19	**2.63 ± 0.16** *	**2.21 ± 0.13** ***	**1.69 ± 0.13** ***
MHCII B-cells (MFI)	1453.80 ± 44.10	1334.60 ± 89.70	1235.60 ± 111.64	**1093.20 ± 94.51** *
MHCII DCs (MFI)	4355.40 ± 77.92	4141.40 ± 112.06	4003.00 ± 145.61	**3854.60 ± 88.79** *
CD86 B-cells (MFI)	273.20 ± 7.98	**341.20 ± 16.00** **	280.80 ± 10.49	302.60 ± 14.79
CD86 DCs (MFI)	1991.20 ± 92.66	1733.80 ± 46.13	**1677.40 ± 60.65** *	1754.60 ± 67.69

Values are expressed as the means (±SE) for each group (n = 5 mice/group).

* $p < 0.05$

** $p < 0.01$

*** $p < 0.001$.